

# The temporal and spatial organization of HIV-1 production in macrophages

## **Dissertation**

Zur Erlangung der Würde des Doktors der Naturwissenschaften  
des Fachbereichs Biologie, der Fakultät für Mathematik, Informatik und Naturwissenschaften,  
der Universität Hamburg

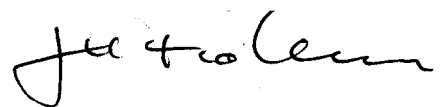
vorgelegt von

**Herwig Koppensteiner**  
aus Linz, Österreich

Hamburg 2012

Genehmigt vom Fachbereich Biologie  
der Fakultät für Mathematik, Informatik und Naturwissenschaften  
an der Universität Hamburg  
auf Antrag von Prof. Dr. T. DOBNER  
Weitere Gutachterin der Dissertation:  
Priv.-Doz. Dr. N. FISCHER  
Tag der Disputation: 13. April 2012

Hamburg, den 29. März 2012



Professor Dr. J. Fromm

Vorsitzender des Promotionsausschusses  
Biologie

Die vorliegende Arbeit wurde in der Zeit von März 2009 bis März 2012 unter Anleitung von Dr. Michael Schindler und Prof. Dr. Thomas Dobner und Betreuung durch PD Dr. Nicole Fischer am Heinrich-Pette-Institut - Leibniz-Institut für Experimentelle Virologie in der Arbeitsgruppe für Viruspathogenese angefertigt.

Teile dieser Arbeit wurden bereits veröffentlicht:

**Koppensteiner, H., Banning, C., Schneider, C., Hohenberg, H., and Schindler, M.** (2012) Macrophage internal HIV-1 is protected from neutralizing antibodies. *J Virol* 86: 2826-2836

1. Gutachter: Prof. Dr. Thomas Dobner

2. Gutachter: PD Dr. Nicole Fischer

Termin der mündlichen Prüfung: 13.04.2012

# Inhalt

<b>Zusammenfassung .....</b>	<b>4</b>
<b>Summary.....</b>	<b>4</b>
<b>1 Introduction .....</b>	<b>6</b>
<b>1.1 Human Immunodeficiency Virus Type 1: origin and epidemiology .....</b>	<b>6</b>
<b>1.2 Morphology and genome organization of HIV-1.....</b>	<b>8</b>
<b>1.3 HIV-1 replication cycle .....</b>	<b>9</b>
<b>1.4 AIDS pathogenesis .....</b>	<b>10</b>
<b>1.5 The role of macrophages in the context of HIV-1 .....</b>	<b>11</b>
1.5.1 CCR5- and CXCR4- tropism .....	12
1.5.2 Macrophages are HIV-1 reservoirs.....	12
1.5.3 HIV-1 affects the central nervous system .....	13
1.5.4 The virological synapse.....	14
1.5.5 Intracellular HIV-1 and the Trojan exosome hypothesis.....	15
<b>1.6 Tetraspanins and their functions during HIV-1 infection.....</b>	<b>16</b>
<b>1.7 Aims of the study.....</b>	<b>19</b>
<b>2 Materials.....</b>	<b>20</b>
<b>2.1 Eukaryotic cell lines .....</b>	<b>20</b>
<b>2.2 Bacteria.....</b>	<b>20</b>
<b>2.3 Media.....</b>	<b>20</b>
2.3.1 Media for bacteria.....	20
2.3.2 Media for cell culture .....	20
<b>2.4 Nucleic acids.....</b>	<b>21</b>
2.4.1 Oligonucleotides for site-directed mutagenesis .....	21
2.4.2 Plasmids.....	21
2.4.3 DNA ladder .....	21
2.4.4 Nucleotides for Polymerase-chain-reaction.....	21
<b>2.5 Enzymes .....</b>	<b>22</b>
2.5.1 Restriction endonucleases.....	22
2.5.2 Other enzymes .....	22
<b>2.6 Antibodies.....</b>	<b>22</b>
2.6.1 Primary antibodies .....	22
2.6.2 Secondary antibodies .....	22
<b>2.7 Reagents .....</b>	<b>22</b>
2.7.1 Chemicals.....	22
2.7.2 Reagent systems (Kits).....	23
<b>2.8 Buffer and solutions.....</b>	<b>23</b>

2.9	Laboratory equipment .....	24
<b>3</b>	<b>Methods .....</b>	<b>25</b>
3.1	<b>Molecular biological methods .....</b>	<b>25</b>
3.1.1	DNA-standard methods.....	25
3.1.2	Transformation of <i>E. coli</i> One Shot® Top10 .....	25
3.1.3	Isolation of plasmid-DNA.....	25
3.1.4	Isolation of DNA from agarose gels.....	26
3.1.5	Polymerase chain reaction (PCR) .....	26
3.1.6	Sequencing .....	26
3.1.7	Generation of HIV-1 provirus and expression vectors .....	26
3.2	<b>Cell biological methods .....</b>	<b>28</b>
3.2.1	Cultivation of adherent and suspension cell .....	28
3.2.2	Isolation of mononuclear cells from peripheral blood.....	28
3.2.3	Generation of virus stocks by calcium phosphate transfection of 293T cells .....	28
3.2.4	HIV-1 p24 capsid antigen-ELISA.....	29
3.2.5	Infectivity assay .....	29
3.2.6	Infection of monocyte derived macrophages .....	29
3.2.7	Co-cultivation experiments .....	29
3.2.8	FACS-based FRET assay.....	30
3.2.9	Nucleofection of monocyte derived macrophages .....	30
3.3	<b>Microscopy.....</b>	<b>30</b>
3.3.1	Live-cell microscopy .....	30
3.3.2	TIRF microscopy.....	30
3.3.3	Confocal fluorescence microscopy and staining .....	31
3.3.4	Correlative transmission electron microscopy.....	31
3.4	<b>Imaging analysis and software .....</b>	<b>32</b>
<b>4</b>	<b>Results .....</b>	<b>33</b>
4.1	<b>Generation and characterization of a macrophage tropic HIV-1 with an internal GFP-tag in the HIV-1 Gag polyprotein .....</b>	<b>33</b>
4.1.1	Characterization of pBR-NL4-3-V3 92th014.12_Gag-iGFP (HIV-1 GG).....	34
4.2	<b>In HIV-1 infected macrophages Gag accumulates intracellular.....</b>	<b>36</b>
4.3	<b>The temporal origin of macrophage internal Gag accumulations .....</b>	<b>37</b>
4.4	<b>Absence of assembly sites at the plasma membrane of HIV-1 infected macrophages...</b>	<b>39</b>
4.5	<b>HIV-1 within VCC are inaccessible to antibodies.....</b>	<b>42</b>
4.6	<b>HIV-1 is efficiently transferred from macrophages to T-cells.....</b>	<b>46</b>
4.7	<b>The spatial organization of an internal Gag accumulation .....</b>	<b>48</b>
4.8	<b>Gag alone is able to form VCC-like expression pattern .....</b>	<b>50</b>
4.9	<b>Gag interacts with tetraspanins found in VCCs.....</b>	<b>51</b>
<b>5</b>	<b>Discussion .....</b>	<b>52</b>
5.1	<b>HIV-1 Gag assembles in intracellular virus containing compartments .....</b>	<b>53</b>

5.2	Virus containing compartments are protected from antibodies.....	54
5.3	Neutralizing antibodies cannot prevent HIV-1 cell-to-cell transfer.....	55
5.4	HIV-1 is sequestered into a macrophage internal membranous web.....	56
5.5	Gag interaction with tetraspanins might be sufficient to induce intracellular accumulations in macrophages .....	58
6	Conclusion.....	60
7	References .....	62
	List of Figures .....	72
	Abbreviations.....	73
	Danksagung .....	76
	Eidesstattliche Erklärung.....	77

## Zusammenfassung

Makrophagen sind wichtige Zielzellen für das Humane Immundefizienzvirus Typ 1 (HIV-1) und überleben eine Infektion über Wochen und sogar Monate. Während dieser Zeit produzieren Makrophagen ständig neue Viren und bilden ein Reservoir für HIV-1. Makrophagen tragen HIV-1 auch über die Blut-Hirn-Schranke ins Zentrale Nervensystem, was zu schweren neurologischen Schäden führen kann. Der Replikationszyklus von HIV-1 in Makrophagen unterscheidet sich von dem in T-Zellen; vor allem die späte Phase der Replikation, der Zusammenbau des Partikels und dessen Freisetzung, ist unklar. Im Gegensatz zu T-Zellen akkumulieren Makrophagen HIV-1 in intrazellulären membranumschlossenen Kompartimenten, englisch genannt *virus containing compartments* (VCC). Während der Ursprung dieser Strukturen kontrovers diskutiert wird, könnte die Akkumulation von HIV-1 in VCCs einen Schutz vor dem Immunsystem darstellen, weil sich das Virus in einer internen Nische befindet, die von außen schwer zugänglich ist. Doch bis jetzt gibt es keine Beweise, dass Viren, die sich in diesen VCCs befinden, vor dem humoralen Immunsystem des Wirtes geschützt sind.

Um die Entstehung von VCCs und ihre potentielle Zugänglichkeit für Antikörper zu untersuchen, wurde ein HIV-1 Konstrukt hergestellt, dessen Strukturprotein Gag mit dem Grün-fluoreszierenden Protein (GFP) markiert ist und in primären Makrophagen replizieren kann. Lebendzellmikroskopie zeigte zu frühen Zeitpunkten eine schwache Expression von Gag im Zytoplasma, gefolgt von großen intrazellulären Gag Akkumulationen, die über Stunden und sogar Tage stabil blieben. Zusätzliche Untersuchungen mittels „Total internal reflection fluorescence (TIRF)“ Mikroskopie, eine Methode, mit der selektiv die Membran von Zellen visualisiert werden kann, lieferten keine Hinweise für die HIV-Assemblierung an der Plasmamembran von Makrophagen. Durch die Verwendung von verschiedenen neutralisierenden Antikörpern konnte zum ersten Mal gezeigt werden, dass HIV-1 in Makrophagen nicht durch Antikörper neutralisiert werden kann. Die Unzugänglichkeit der VCCs für Antikörper wurde dadurch untermauert, dass HIV-1 von Antikörper behandelten Makrophagen erfolgreich auf T-Zellen durch Zell-zu-Zell Transfer übertragen werden konnte.

Durch die 3D-Rekonstruktionen von elektronmikroskopischen Serienschritten konnte gezeigt werden, dass Gag Akkumulationen viralen Partikeln entsprechen, die sich in umschlossenen Kompartimenten befinden und um ein membranöses Netz gruppiert sind. Obwohl manche dieser VCCs mit der Plasmamembran verbunden sind, scheint die komplexe Membranarchitektur der VCCs die viralen Partikel vor neutralisierenden Antikörpern abzusichern.

Die Ergebnisse dieser Arbeit zeigen, dass HIV-1 in einem intrazellulären membranösen Netz der Makrophagen entsteht, wo das Virus vor der humoralen Immunantwort des Wirtes geschützt ist, aber trotzdem sehr effizient an T-Zellen über Zell-zu-Zell Transfer weitergegeben werden kann.

## Summary

Macrophages are important Human Immunodeficiency Virus Type 1 (HIV-1) target cells and survive an infection for several weeks and months. During this period macrophages constantly produce new virions and serve as a reservoir for HIV-1. In addition, macrophages are transport vehicle for the virus into the central nervous system and the brain leading to severe neurological diseases. The replication cycle of HIV-1 in macrophages differs substantially from that in T-cells and especially the late steps comprising assembly and release are unclear. In contrast to T-cells, macrophages accumulate HIV-1 in intracellular membrane enclosed compartments, designated virus containing compartments (VCCs). Controversy exists regarding the origin of these structures and if they might represent an immune evasion mechanism of HIV-1. Theoretically, the virus could be protected from neutralizing antibodies by sequestration into an internal niche, which is difficult to access from the exterior. However, until now, evidence of whether internal virus accumulations are protected from the host's humoral immune response is still lacking.

To investigate the formation and antibody accessibility of VCCs, HIV-1 with green fluorescent protein (GFP)-tagged Gag able to replicate in primary macrophages was generated during this thesis. Live-cell microscopy showed faint initial cytosolic Gag expression followed by large intracellular Gag accumulations, which stayed stable for hours and even days. Additionally, total internal reflection fluorescence (TIRF) microscopy revealed the absence of HIV-1 assembly sites from the plasma membrane of macrophages. Using different neutralizing antibodies it was demonstrated for the first time that macrophage internal HIV-1-containing compartments cannot be targeted by neutralizing antibodies. Furthermore, antibody treated macrophages efficiently transferred HIV-1 from VCCs to adjacent T-cells via cell-to-cell transfer.

Three dimensional reconstruction of electron microscopic slices revealed that Gag accumulations correspond to viral particles within enclosed compartments. These are grouped or in close contact to a membranous web. Thus, although some VCCs were connected to the plasma membrane, the complex membrane architecture of the HIV-1-containing compartment might shield viral particles from neutralizing antibodies.

In sum, this thesis provides evidence that HIV-1 is sequestered into a macrophage internal membranous web, in which the virus is protected from the humoral immune response, but can be efficiently transmitted to T-cells via cell-to-cell contact.



# 1 Introduction

## 1.1 Human Immunodeficiency Virus Type 1: origin and epidemiology

More than 30 years have gone since in 1981 the Center of Disease Control and Prevention (CDC) reported the first cases of young homosexual men in Los Angeles who suffered from a new disease named acquired immunodeficiency syndrome (AIDS) with unknown origin (De Cock et al., 2011). Only two years later the group of Luc Montagnier published their successful isolation of a new human retrovirus from AIDS patients that replicated in human T-cells (Barré-Sinoussi et al., 1983). They could also visualize the virus using electron microscopy and gave the origin of AIDS a face. For these investigations Françoise Barré-Sinoussi and Luc Montagnier were awarded the Nobel Prize in Medicine in 2008. In 1985 the first ELISA assay for the detection of antibodies against the new retrovirus was available and in 1986 it was defined as a member of the lentivirus family and named Human Immunodeficiency Virus Type 1 (HIV-1) (Coffin et al., 1986, De Cock et al., 2011). In the same year the related Human Immunodeficiency Virus Type 2 (HIV-2) was isolated from African AIDS patients (Clavel et al., 1986). HIV-1 exerts large variability and is categorized into four different groups. The main causative agent of the AIDS pandemic is group M. Some cases of AIDS are caused by another group of HIV-1, called O (named for “outliers”), which was discovered in 1990. HIV-1 O is less prevalent than M and causes only 1% of HIV-1 infections worldwide – all in east central Africa. In 1998 another new group of HIV-1 was discovered and named group N (non-M non-O). This strain is even less prevalent than HIV-1 O and was only found in 13 cases in Cameroon. Recently, HIV-1 group P was described and only found in 2 persons thus far. (Sharp and Hahn, 2011; Cao and Walker, 2000)

Work in this thesis covers HIV-1 group M, since it is the predominant strain causing the AIDS pandemic. For simplification HIV-1 group M will be abbreviated HIV-1.

HIV-1 was a cross-species transmission of the related Simian Immunodeficiency Virus (SIV) from chimpanzees (SIVcpz) to humans in central Africa in the early 20<sup>th</sup> century, where people hunt and eat monkeys. Then the virus adapted to humans and was efficiently transmitted by sexual intercourse and contaminated blood products (De Cock et al., 2011, Bailes et al., 2003). It is unknown when HIV-1 reached the Western countries, but retrospective analyses of blood samples indicated that HIV-1 spread to Haiti in the 1960s and then to the USA (Sharp and Hahn, 2011). Initially it was believed that homosexual men and injecting drug users are the major group which were at risk of being infected. Today it is known that HIV-1 can also be efficiently transmitted by heterosexual contacts, blood transfusions and mother to child transmission (prenatal or during birth or by breast feeding) (Hoffmann et al., 2008).

The yearly UNAIDS report of 2010 showed that 2009 33.4 million people were infected with HIV-1, among them 2.1 million children under the age of 15 years. 2.7 million were newly infected in 2009 and 2 million died of AIDS (UNAIDS report 2010; AIDS epidemic update: November 2009). The number of people living with HIV-1 still rises, whereas new infections and AIDS related deaths decreased in the last years. The introduction of antiretroviral therapy (ART) 15 years ago made infection with HIV-1 a treatable disease, but it is still not possible to cure the patients (De Cock et al., 2011). Figure 1.1 shows the unequal global distribution of HIV-1. The continent which is most dramatically affected by HIV-1 is Africa, especially the sub-saharian region. About one sixth of the world's HIV-1 infected people are living in South Africa, mainly due to the fatal HIV-1 management by the former government of Thabo Mbeki, who denied HIV-1 as the cause of AIDS. (UNAIDS report 2010, De Cock et al., 2011)

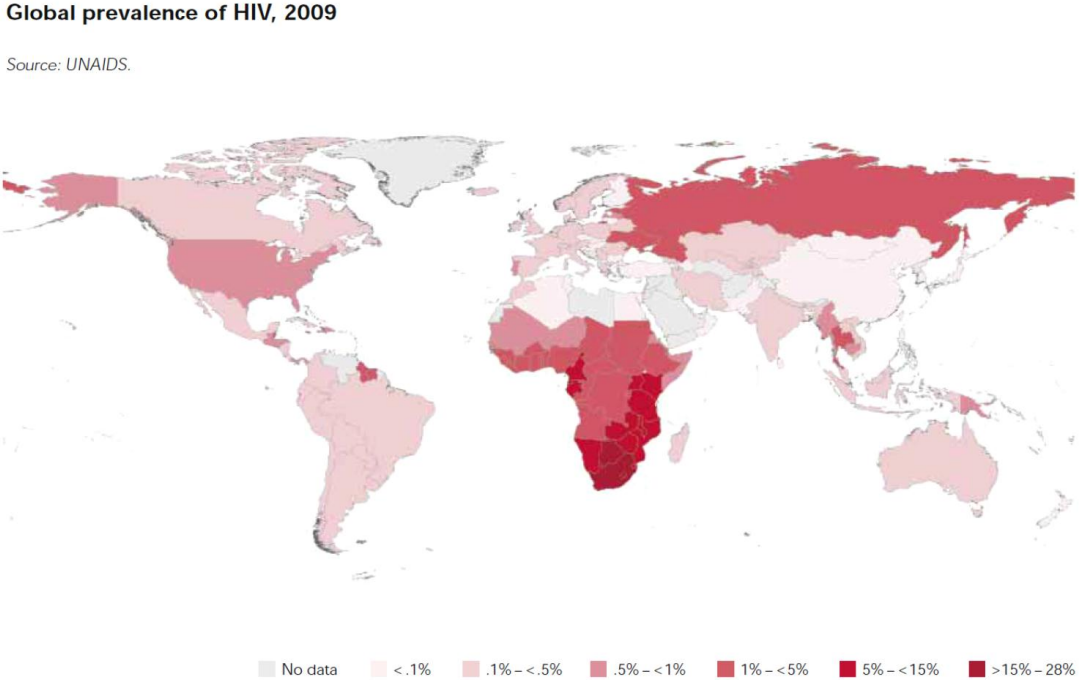


**Figure 1.1 Global prevalence of HIV-1.** (UNAIDS Report 2010)

## 1.2 Morphology and genome organization of HIV-1

HIV-1 is a membrane enveloped retrovirus and a member of the genus *Lentiviridae* that has a diameter of about 100 nm. Lentiviruses have the unique capacity to infect non-dividing cells (Waki and Freed, 2010). Figure 1.2 shows the structure of the viral particle and the genome organization of HIV-1. Its RNA-genome encodes for 3 polyproteins Gag, GagPol and Gp160 (Env) as well as for the regulatory proteins Tat and Rev, and for the accessory proteins Vif, Vpr, Vpu and Nef. Env is cleaved by cellular proteases into Gp120 [SU] and Gp41 [TM] and is glycosylated. The Gag- and the GagPol polyproteins are incorporated into the immature virion and cleaved during a maturation step by the viral protease (PR) into the Gag subunits MA, CA, NC, p6 and the pol subunits IN, RT and PR (Frankel and Young, 1998). Gag is the main structural protein of the virus and Gag by itself is able to form virus like particles (Gousset et al., 2008; Waki and Freed, 2010).

Two single stranded positive RNA copies of the viral genome, which has a size of 9.5kB and is flanked by 5' and 3' long terminal repeats (LTR), are incorporated into the virus particle. The promoter for transcription by the RNA-polymerase II is located in the 5' LTR. Inside the virion the RNA is associated with the p7 nucleocapsid (NC), a subunit of Gag. The conical capsid is built by p24 capsid proteins (CA) and harbors the viral genome, the Pol subunits protease (PR), integrase (IN) and reverse transcriptase (RT) as well as the accessory proteins Vif, Vpr and Nef. In addition, the fourth Gag subunit p6 is encapsulated by the virion, whereas the regulatory proteins (Rev and Tat) and the accessory protein Vpu are not packaged. P17 matrix (MA) forms the inner coat of the virion which is enveloped by a cellular phospholipid bilayer in which the Gp120-Gp41 complexes are integrated. (Frankel and Young, 1998)

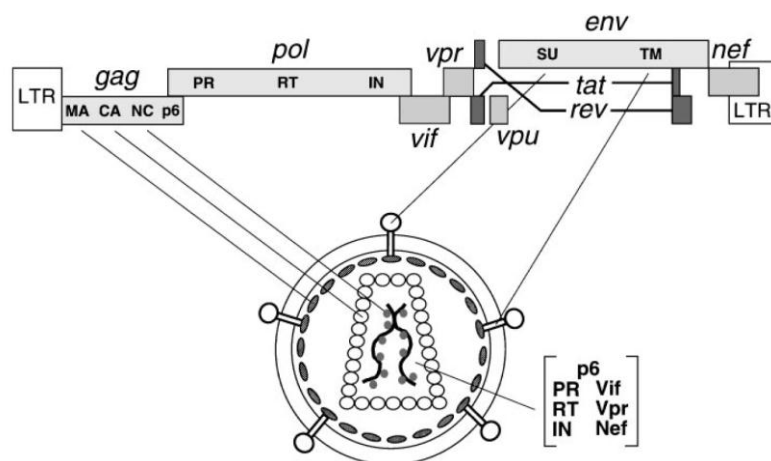


**Figure 1.2 Structure and genome organization of HIV-1.**

(Frankel and Young, 1998)

### 1.3 HIV-1 replication cycle

The Human Immunodeficiency Virus Type 1 infects mainly CD4<sup>+</sup> T-cells and macrophages. This CD4 tropism is due to the fact that HIV-1 uses this surface receptor for entry. The binding of HIV-1 Gp120 to CD4 leads to a conformational change in Gp120 that opens the binding site of Gp120 to the chemokine coreceptor (mainly CCR5 or CXCR4). Due to the coreceptor binding the virus fuses with the cellular membrane and the nucleocapsid enters the cell while being disintegrated. In the cytosol the virion associated reverse transcriptase is activated and synthesizes the viral cDNA (Monini et al., 2004). The viral cDNA within the preintegration complex (PIC) is transported into the nucleus. Although the exact mechanisms are not fully understood, members of the lentiviral subgroup are the only retroviruses which are able to infect non-dividing cell types (Carter and Ehrlich, 2008). In the nucleus the viral genome is integrated into the host-cell genome by the HIV-1 integrase. The first viral protein translated is Tat that binds to the TAR element of the viral promoter and enhances the transcription of the viral cDNA (He and Zhou, 2011). This leads to the production of genomic (unspliced) and messenger (spliced) RNAs which are transported into the cytoplasm by the help of the viral Rev protein (Grewe and Überla, 2010).

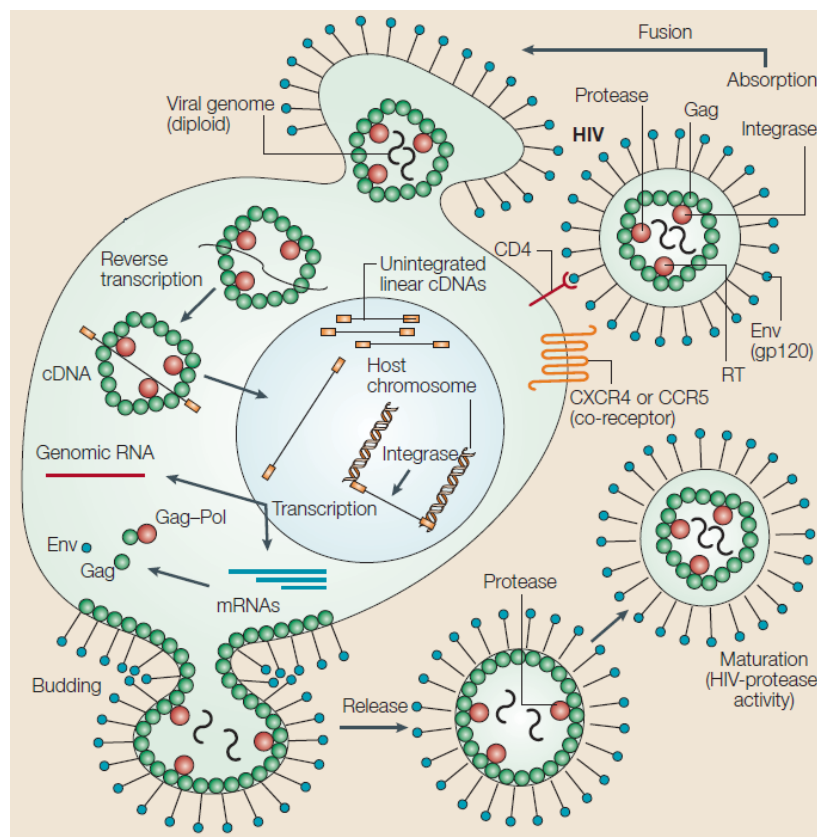


Figure 1.3 Replication cycle of HIV-1.

(Monini et al., 2004)

Translation of viral mRNA leads to the production of Gag-, GagPol- and Env- polyproteins and the accessory proteins Vif, Vpr, Vpr and Nef. In CD4+ T-cells and most cell lines assembly of viral particles takes place at the plasma membrane, where a lot of different cellular proteins are recruited and form the so called budding machinery. The exact mechanism is matter of intense investigations (Waki and Freed, 2010). The virus buds through tetraspanin-enriched-microdomains fused with lipid rafts at the host's plasma membrane where also the viral Gp120-Gp41 complex is located (Hogue et al., 2011). During this process the Gag- and the GagPol polyproteins, the viral genomic RNA and the viral proteins Vif, Vpr and Nef form the immature virion. The viral envelope is derived from the plasma membrane of the host-cell, thus containing a large variety of cell surface molecules next to the viral Gp41-Gp120 proteins (Chertova et al., 2006). Shortly post release of the immature viral particle the protease cleaves Gag and the GagPol polyproteins. By regrouping the Gag-subunits to the conical capsid the virus matures and becomes infectious. (Monini et al., 2004; Frankel and Young, 1998; Waki and Freed, 2010)

### **1.4 AIDS pathogenesis**

A few weeks post HIV-1 infection most people develop an acute retroviral syndrome. These symptoms are often misdiagnosed for acute infectious mononucleosis or viral hepatitis (Khan and Walker, 1998; Pantaleo et al., 1993). During this acute phase the amount of CD4+ T-cells decline while the viral load in the blood rises dramatically. Generally the virus can be suppressed by the immune system and CD4+ T-cell counts recover within four weeks (Cao and Walker, 2000; Hoffmann et al., 2008 2008; Pantaleo et al., 1993). This effective suppression of HIV-1 at the end of the acute phase could be due to cytotoxic CD8+ T-cells, but also HIV-1 specific antibodies can be detected at this time (4 weeks after the exposure) (Cao and Walker, 2000; Hoffmann et al., 2008). Subsequently, viral loads and CD4+ T-cell counts may stay stable for years with HIV-1 mainly persisting in lymph nodes and other cellular reservoirs. Viral loads during the asymptomatic phase predict disease progression; lower viremia is associated with the best progression (Cao and Walker, 2000; Mellors et al., 1997). The cellular and humoral immune response suppresses the virus over a long period of time during this chronic phase (Cao and Walker, 2000).

Nevertheless, CD4+ T cell counts slowly decrease due to ongoing direct or indirect cytotoxic effects induced by HIV-1. This phase of HIV-1 pathogenesis normally takes years, in general over a median period of 10 years (Cao and Walker, 2000; Pantaleo et al., 1993). When blood CD4+ T-cells fall under the level of 200 T-cells/ $\mu$ l, the patient has reached the phase of AIDS with symptoms of immune deficiency and a dramatic rise of virus titers (Hoffmann et al., 2008). Immune system dysfunction also leads to a non-functional immune response against other pathogens like viral, bacterial, fungal and parasitic infections and also rare cancers like the Kaposi Sarcoma can be developed (Barré-Sinoussi et

al., 1983; Hoffmann et al., 2008; Pantaleo et al., 1993). These so called opportunistic diseases cause the death of the patient within months to few years.

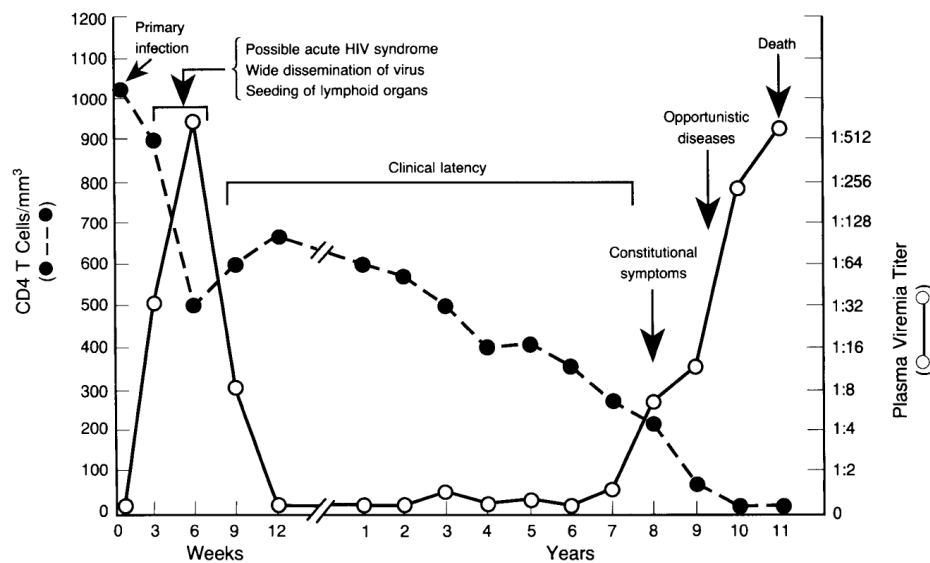


Figure 1.4 Typical course of HIV-1 infection.

(Pantaleo et al., 1993)

This deadly course of disease progression can be prevented by the use of antiretroviral therapy (ART). By the combination of different antiretroviral drugs (nucleosidic- and non-nucleosidic reverse transcriptase inhibitors, protease inhibitors, entry inhibitors and integrase inhibitors) it is possible to suppress viral loads under the detection level and expand the chronic phase theoretically to the natural end of patient's life. However, it is not yet possible to cure patients and eliminate all HIV-1 reservoirs. Furthermore, severe side effects of ART (e.g. lipodystrophy caused by protease inhibitors) are a serious problem of the actual therapy (Hoffmann et al., 2008).

### 1.5 The role of macrophages in the context of HIV-1

Macrophages are terminally differentiated, non-dividing cells, derived from monocytes. They represent a distinct population of phagocytes which are found under different names in various tissues (e.g. microglia in the brain, alveolar macrophages in the lung or Kupffer cells in the liver) (Waki and Freed, 2010; Benaroch et al., 2010). Macrophages play an important role in both branches of the immune system, in the innate and adaptive immune response. They phagocyte cellular debris and pathogens, but also act as professional antigen presenting cells (APC) presenting peptides of lysed pathogens via the MHC-II pathway to CD4+ T-cells (Gordon and Taylor, 2005; Benaroch et al., 2010). Macrophages can have a life span of several weeks to months, patrol mucosal surfaces, infiltrate tissues at sites of inflammation and take HIV-1 into the brain, because of their ability to cross the blood-brain barrier (Maung et al., 2011; Waki and Freed, 2010).

### **1.5.1 CCR5- and CXCR4- tropism**

Macrophages are important target cells for HIV-1. In contrast to T-cells macrophages survive the infection with HIV-1 for weeks and months (Welsch et al., 2007; Benaroch et al., 2010; Le Douce et al., 2010). Macrophages and CD4+ memory T-cells are targeted early in the course of disease. This is due to the expression of CCR5 at the surface of macrophages which is used as coreceptor by most sexually transmitted virus strains (Marsh et al., 2009; Waki and Freed, 2010; Maung et al., 2011). In general, HIV-1 can use different chemokine receptors to enter the target cell: mainly CCR5 or CXCR4. CCR5 tropic (R5) isolates are able to infect both macrophages and primary CD4+ T-cells, but fail to replicate in transformed T-cell lines. During disease progression there is a shift in coreceptor tropism and the majority of viruses becomes dual-tropic (R5/X4) and in some cases CXCR4 tropic (X4). These isolates fail to infect macrophages, but can enter transformed T-cell lines (Cao and Walker, 2000; Waki and Freed, 2010). It has been suggested that X4 strains are more sensitive to antibody neutralization than R5 strains (Waki and Freed, 2010). In line with this, the appearance and expansion of X4 viruses correlates with disease progression and enhanced immune deficiency (Connor et al., 1993; Spijkerman et al., 1998). The importance of CCR5 in the context of HIV-1 is shown by the fact that a deletion of 32 base pairs in the CCR5 gene (CCR5 $\Delta$ 32) leads to full protection against HIV-1, if the mutation is homozygous (Dean et al., 1996; Cao and Walker, 2000; Maung et al., 2011; Allers et al., 2011). This finding was even strengthened in 2009 by the first ever documented patient who was “cured” from an HIV-1 infection. An HIV-1 infected patient with an additionally acute myeloid leukemia underwent hematopoietic stem cell transplantation with a graft consisting of CCR5 $\Delta$ 32 donor cells. After transplantation viral loads decreased under the detection level and the CD4+ T-cell counts relapsed (Hütter et al., 2009; Allers et al., 2011). The importance of CCR5 as major HIV-1 coreceptor also led to the invention of a new class of antiretroviral drugs: CCR5 antagonists that inhibit the entry of HIV-1 into the target cell (Gulick et al., 2008).

### **1.5.2 Macrophages are HIV-1 reservoirs**

Using ART viral loads can be suppressed under the detection level within 2 weeks of treatment (Pierson et al., 2000). Thus it was postulated that during long term ART virtually all HIV-1 infected cells will die, which would subsequently cure the infection (Hoffmann et al., 2008, Pierson et al., 2000). Unfortunately it became evident that HIV-1 persists in so called long term reservoirs, which consist of latently infected resting CD4+ T-cells with integrated provirus (Pierson et al., 2000), dendritic cells and macrophages within the lymph nodes and in bone marrow haematopoietic stem cells (Le Douce et al., 2010). This leads to a dramatic increase of viral load if the therapy is stopped or interrupted. Therefore, HIV-1 infected patients have to be treated with ART for their whole life.

Macrophages might play a role in boosting HIV-1 infection after stopping ART. Macrophages can store high amounts of unintegrated viral DNA in circular form and infected macrophages were found in lymph nodes of ART treated HIV-1 patients with viral loads under the detection limit (Le Douce et al., 2010). Additionally it has been reported, that macrophages have some cellular HIV-1 restriction mechanisms that are not found in T-cells, e.g. high amounts of tetherin and SAM-HD1 (Schindler et al., 2010; Laguette et al., 2011). The adaptation of HIV-1 to these restrictions further indicates that macrophages play an important role in HIV-1 pathogenesis.

### **1.5.3 HIV-1 affects the central nervous system**

HIV-1 infection of the central nervous system (CNS) can lead to severe HIV associated neurocognitive disorders (HAND), for example HIV associated dementia (HAD) and pathological HIV encephalitis (HIVE) (Maung et al., 2011; Schnell et al., 2011; Thompson et al., 2011). Progression of these neurological disorders is decelerated but not prevented by ART. The bioavailability of antiretroviral drugs in the CNS is low. Thus, viral reservoirs in the CNS cannot be efficiently targeted by ART. Since life expectancy of HIV-1 infected patients under regimen increases, there is a growing risk for development of neurological diseases (Schnell et al., 2011). HIV-1 strains isolated from the cerebrospinal fluid of HAD patients use CCR5 as coreceptor (Maung et al., 2011; Schell et al., 2011). In 2009 the group of McLean published their study of SIV infected macaques sacrificed at different time points. By the use of laser-microdissection they isolated pure perivascular macrophages, parenchymal microglia, and astrocyte populations from the brain of the animals. HIV-1 which was found in the brain early after infection was predominantly located in perivascular macrophages (Thompson et al., 2009). These findings support the “Trojan horse” model postulating that HIV-1 infected macrophages transport the virus over the blood-brain barrier into the CNS. Within this niche HIV-1 forms a reservoir which is largely protected from antiviral therapy (Thomson et al., 2009, Clay et al., 2007). Recently these findings could be confirmed in humans by the isolation of pure perivascular macrophages, parenchymal microglia, and astrocyte from the brain tissues of five untreated HIV-1 positive individuals who died during the presymptomatic stage of infection due to non HIV-related reasons (Thompson et al., 2011). In addition, stimulation of macrophages in the CNS by Gp120 leads to the release of neurotoxins, including excitotoxins, chemokines and pro-inflammatory cytokines that cause neuronal injury and death (reviewed in Maung et al., 2011). During disease progression the percentage of infected perivascular macrophages in the CNS correlates with the development of HAND and inversely with peripheral blood CD4 counts (Maung et al., 2011; Thompson et al., 2011).



#### 1.5.4 The virological synapse

HIV-1 can be spread to uninfected cells either by “classical” fluid-phase diffusion of viral particles or by direct cell-cell transfer. Both X4 and R5 strains are reported to be able to spread between T-cells by cell-cell transfer (Martin et al., 2010). These contact sites between cells through which virus can be transferred from an infected to an uninfected cell is called virological synapse (VS), in reference to the immunological synapse between an APC and a T-cell (Jolly and Sattentau, 2007). Some studies showed that cell-to-cell spread is far more efficient than cell free infection, although the exact mechanism is a matter of intense debates (reviewed by Waki and Freed, 2010). Cell-to-cell spread might be important for the spread of HIV-1 *in vivo* especially in lymph nodes and other lymphatic organs. Hübner and colleagues published 3-dimensional movies of GFP tagged virions being transferred via VS to uninfected T-cells. The transfer by VS was very efficient (9.3% new infected T-cells after 48h) compared with infection when cell-to-cell transfer was inhibited by a 0.4µm transwell barrier (0.4% new infected T-cells after 48h) (Hübner et al., 2009). In addition cell-to-cell spread in T-cells depends on Gp120-Gp41 and its interaction with CD4 (Jolly and Sattentau, 2007; Hübner et al., 2009). Different virus families e.g. herpesviruses, poxviruses and hepatitis C virus use cell-to-cell transfer to evade the immune system, because the involved tight junctions are impermeable for antibodies (Favoreel et al., 2006; Law et al., 2002; Timpe et al., 2008). This fact leads to speculations that HIV-1 also uses VS to evade the immune system (Waki and Freed, 2010). This hypothesis was strengthened by reports derived from dendritic cells. These use VS for the transfer of captured HIV-1 to T-cells in *trans*, and this transfer is resistant to neutralizing antibodies (Ganesh et al., 2004; van Montfort et al., 2007). However, it was shown that both cell-to-cell spread and cell free infection between T-cells are sensitive to entry inhibiting neutralizing antibodies. Using electron tomographic reconstruction of contacts between infected and uninfected T-cells it was demonstrated, that VS between T-cells are relative loose structures which are not closed or inaccessible. Thus, newly synthesized virions are released into the space between T-cell VS (Martin et al., 2010).

Less is known on the formation of VS between macrophages or between macrophages and T-cells. The most important studies in this context are two papers from 2008; one of the Freed lab and one of Sattentau’s group (Gousset et al., 2008; Groot et al., 2008). The group of Freed used an HIV-1 construct that has a tetra-cys tag inside the Gag polyprotein allowing to visualize rapid Gag movement from the infected macrophage to the contact site with a T-cell. Env was not required for VS formation or Gag movement to the VS of macrophages (Gousset et al., 2008). Groot and colleagues used a coculture of infected macrophages and autologous CD4+ T-cells with or without different inhibitors and with or without a 0.3µm transwell to measure cell free infection rates. First they could verify that cell-to-cell transfer (8-9% infected T-cells after 10h) is more efficient than cell free infections (0.5% infected T-cells after 10h). Interestingly they disagree with the Freed study and

show that Gp120-CD4 interaction is essential for cell-to-cell transfer of HIV-1 and to a lower level also Gp120-CCR5 interaction (Groot et al., 2008). In this context it is important to distinguish between the formation of VS, where Env seems not to be involved and in the transfer of HIV-1 by VS, where Env seems to be important. Although these studies suggest that macrophage VS and T-cell VS are similar, further investigations will analyze the formation, function and *in vivo* relevance of VS.

### **1.5.5 Intracellular HIV-1 and the Trojan exosome hypothesis**

Since the late 1980s it is known that in infected macrophages HIV-1 particles as well as budding events can be found in membrane enclosed compartments that seem to be intracellular (Gendelman et al., 1988). But the origin and the fate of these virus containing compartments (VCCs) remained a matter of intense debates due to the fact that they could only be visualized by electron microscopical analyses. Immune electron microscopy studies showed that VCCs contained markers of late endosomes or multi vesicular bodies (MVB): MHC-II and the tetraspanins CD63, CD53, CD9, CD81 and CD82 (Raposo et al., 2002, Pelchen-Matthews et al., 2003, Deneka et al., 2007). These findings lead to the idea that VCCs are late endosomes or connected to the late endosomal pathway. Thus, the Trojan exosome hypothesis suggests that VCCs follow an exosome-like pathway to the plasma membrane where its fusion with the plasma membrane leads to the release of the stored viral particles (Gould et al., 2003). Thereby, virions could be protected from the immune system while internal storage represents a mechanism of reservoir establishment within macrophages. This hypothesis was strengthened by the same group showing that the host-protein composition of macrophage produced HIV-1 particles is similar to that of exosomes (Nguyen et al., 2003). The group of Freed designed an HIV-1 construct with mutated Gag (29/31 KE) which was able to bud at the limiting membrane of MVB in T-cells and lots of cell lines, demonstrating that HIV-1 is able to bud into MVBs (Joshi et al., 2009). Since acidification of VCCs would lead to fusion with lysosomes and consequently HIV-1 degradation, the virus evolved mechanisms to prevent acidification of VCCs (Jouve et al., 2007).

The Trojan exosome hypothesis of virus filled MVBs was challenged in 2006 when it was reported that virus release was unaffected when late endosome motility was blocked (Jouvenet et al., 2006). A year later the groups of Kräusslich and Marsh stained infected macrophages during fixation with the membrane impermeant dye ruthenium red (RR), and looked at virus containing structures by electron microscopy (Deneka et al., 2007; Welsch et al., 2007). At least some of the structures were positive for RR, indicating that VCCs have a connection to the plasma membrane or are membrane invaginations. 3D reconstruction of VCCs analyzed by Ion-Abrasion Scanning Electron Microscopy (IA-SEM) showed some VCCs connected to the plasma membrane by narrow tubules, whereas others seemed to have no connection to the plasma membrane (Bennett et al., 2009). Deneka et al.

described this compartment as “intracellular plasma membrane” which is positive for the tetraspanins CD81, CD9 and CD53 (Deneka et al., 2007). In sum, due to different reports showing a connection of at least some of the VCCs with the cell surface, the idea that HIV-1 is stored in intracellular MVB without plasma membrane contact has to be dismissed (Benaroch et al., 2010).

### **1.6 Tetraspanins and their functions during HIV-1 infection**

In CD4+ T-cells HIV-1 accumulation and budding does not occur all over the plasma membrane but might take place through so called tetraspanin enriched microdomains (TEM) (Nydegger et al., 2006).

Tetraspanins (also named transmembrane four superfamily) are cell surface membrane proteins (Tarrant et al., 2003). This family consists of more than 30 members of transmembrane glycoproteins in humans and conserved homologues could be identified in different species including even insects, sponges and fungi (Martin et al., 2005). Tetraspanins have a cytosolic N- as well as a cytosolic C-terminus and two extracellular loops and one inner loop, connecting the four conserved transmembrane domains that give the family its name (Tarrant et al., 2003; Nydegger et al., 2006). In the major extracellular loop and in the transmembrane domains there are some conserved regions separating tetraspanins from other membrane proteins harboring 4 transmembrane domains (Tarrant et al., 2003). Tetraspanins can be found in every tissue but not every tetraspanin is expressed in every cell type (Martin et al., 2005). For example there are 20 different tetraspanins found at the surface of leucocytes. The main function of tetraspanins seems to be the organization of signal transducing complexes at the cell surface (Tarrant et al., 2003). They are linked to cell signaling, antigen presentation, cell adhesion, migration, cell-cell fusion, cell activation, cytoskeletal reorganization and proliferation (Nydegger et al., 2006; Martin et al., 2005). This wide range of involvements is due to the interaction of tetraspanins with integrins, various members of the Ig superfamily and a lot of other membrane associated proteins e.g. EGFR. Furthermore they interact with other tetraspanins to build TEMs (Martin et al., 2005; Nydegger et al., 2006; Tarrant et al., 2003). The broad spectrum of functions of tetraspanins is also caused by the possibility that the same protein can have different functions in different cell types and the degree of functional overlap between different tetraspanins in the same cell is not fully resolved (Tarrant et al., 2003; Martin et al., 2005). Although tetraspanins are involved in so many different cellular processes it is reported that tetraspanins by itself have no intrinsic enzymatic activity, so they seem to be a group of novel adaptor proteins (Martin et al., 2005). Nevertheless, knock out studies in mice revealed a relatively mild phenotype when different tetraspanins are missing: CD151-null mice had abnormalities in T-cells, platelets, and keratinocytes, CD81-null mice in the CNS, B and T-cells, and in retinal pigment epithelial cells, and CD9-null mice in gametes, smooth muscle cells and in the peripheral nervous system (Martin et al., 2005).

The first tetraspanin which was analyzed in the context of HIV-1 was CD63. In contrast to other members of this family CD63 is mainly located at intracellular vesicles like late endosomes or MVBs and only very few amounts are found at the plasma membrane (Charrin et al., 2009). Despite its intracellular location CD63 is incorporated very efficiently into HIV-1 particles next to other tetraspanins and surface proteins (Ruiz-Mateos et al., 2008). This phenomenon is due to the reported surface upregulation of CD63 in HIV-1 infected cells and CD63 can be found at viral assembly sites, leading to the hypothesis that CD63 is essential for the late stages of HIV-1 replication (Martin et al., 2005). This idea was strengthened by a study of Marsh's lab reporting that in macrophages CD63 is transported to TEMs only in HIV-1 infected cells (Deneka et al., 2007). Additionally, it was demonstrated that antibodies against CD63, but not against other tetraspanins, inhibit HIV-1 infection of macrophages with R5 tropic strains. X4 tropic strains and T-cell infection was not affected by anti-CD63 antibodies (von Lindern et al., 2003). Another study investigated the impact of treatment of target cells with soluble recombinant main extracellular loops of different tetraspanins on HIV-1 infection (Ho et al., 2006). HIV-1 infection of macrophages with R5 tropic strains could be blocked by the main extracellular loops of all tested human tetraspanins, including CD63. Addressing the importance of CD63 in the late stage of HIV-1 infection, especially during assembly and release, CD63 was knocked down in HIV-1 infected macrophages (Ruiz-Mateos et al., 2008). However, CD63 knock-down had no impact on virus release, infectivity or intracellular localization. Further discovery of an HIV-1 strain that failed to recruit CD63 without any detectable phenotype strongly questioned the importance of CD63 in HIV-1 replication. Nevertheless, a potential *in vivo* relevance of CD63 for HIV-1 transmission and pathogenesis cannot be excluded.

Apart from CD63 the tetraspanins CD81 and to a smaller amount CD82 are also incorporated into HIV-1 particles (Grigorov et al., 2009). CD81 and CD82 are expressed in a wide range of cell types, especially in leucocytes, but they are absent from erythrocytes, platelets and neutrophils (Tarrant et al., 2003; Charrin et al., 2009). CD82 is extensively studied in cancer patients and it was demonstrated that its expression protects patients from formation of metastases and its loss correlates with bad prognosis (Charrin et al., 2009). CD81 seems to play a role in the activation of natural killer cells and mast cells, in the cellular composition of the brain, in the development of a Th2 response and in the humoral response in general (Charrin et al., 2009). In the context of HIV-1, Gag and Env colocalized with CD81 and CD82 and to a lesser extent with CD63 at the plasma membrane of infected cell lines (Grigorov et al., 2009). In addition only CD81, CD82 and CD63 were incorporated into the infectious particle, although TEMs harbor other tetraspanins. Interestingly, CA p24 and HIV-1 Gag were only coimmunoprecipitated with antibodies against CD81 and CD82, but not with CD63 antibodies. This indicates that CD63 does not interact with CA p24 or HIV-1 Gag. Anti-CD81 treatment or shRNA knock-down lead to a 3-fold decrease in HIV-1 release, whereas similar

effects were observed for CD82, although to a smaller magnitude. Interestingly, when CD81 was inhibited, produced virions showed increased infectivity. (Grigorov et al., 2009) In sum, these observations suggest that CD81 and CD82 play a role during HIV-1 assembly and/ or the budding process. However, their exact functional role in TEM formation and HIV-1 release is still not fully elucidated.

## 1.7 Aims of the study

Macrophages are important for HIV-1 transmission, establishment of viral reservoirs and contribute to neurological disorders associated with HIV-1. In contrast to T-cells, infected macrophages harbor virus containing compartments (VCC) that seem to be intracellular and contain different markers of multivesicular bodies (MVB). However, the role of these VCCs in formation and maintenance of HIV-1 persistence in macrophages is highly controversial and poorly understood, despite intensive investigations.

At the beginning of this thesis most of the data concerning VCCs was derived from electron microscopy studies or biochemical characterization of the compartment. Thus, nothing was known on the formation and tempo-spatial dynamics of macrophage internal virus accumulations. Furthermore, although postulated in many studies, the role of VCCs in HIV-1 mediated immune evasion was unclear.

Specific aims of the thesis were as follows:

- (i) In order to visualize the dynamics of VCC formation and movement in primary HIV-1 infected macrophages infectious GFP-tagged HIV-1 and live cell microscopy should be established.
- (ii) Perform a comprehensive analysis of VCC generation by different microscopical techniques including TIRF.
- (iii) Clarify the role of VCCs in HIV-1 immune evasion and cell-to-cell transfer by antibody accessibility and neutralization experiments.
- (iv) Characterization of the three dimensional structure of macrophage internal VCCs by combining fluorescence and electron microscopy.
- (v) Assess the potential role of tetraspanins as HIV-1 assembly platform in macrophages.

In sum, the overall goal of this thesis was to shed light on the establishment and dynamics of virus containing compartments in macrophages and their role in protection of HIV-1 from the hosts' humoral immune response.

## 2 Materials

### 2.1 Eukaryotic cell lines

Name	Description	Reference
293T	Human kidney epithelial cell line that has been transformed with <i>Adenovirus Typ 5</i> and express the SV40 ( <i>simian virus 40</i> ) large T-Antigen.	DuBridge et al., 1987
Jurkat-LTRG R5	Human T cell line that express CD4 and CCR5 and a GFP reporter under the control of the HIV-1 LTR	Ochsenbauer-Jambor et al., 2006
CemM7	Human T cell line that express CD4, CCR5 and CXCR4 and a <i>tat</i> -inducible luciferase and GFP reporter under the control of the HIV-1 LTR	Brandt et al., 2002

### 2.2 Bacteria

One Shot® Top10	Chemic competent <i>Escherichia coli</i> F- <i>mcrA</i> $\Delta$ ( <i>mrr-hsdRMS-mcrBC</i> ) $\phi$ 80 <i>lacZ</i> $\Delta$ M15 $\Delta$ <i>lacX74</i> <i>recA1</i> <i>araD139</i> $\Delta$ ( <i>araleu</i> ) 7697 <i>galU</i> <i>galK</i> <i>rpsL</i> (StrR) <i>endA1</i> <i>nupG</i> (Invitrogen, Karlsruhe, Germany)
-----------------	---

### 2.3 Media

#### 2.3.1 Media for bacteria

Luria-Bertani-Medium (LB-Medium)	10 g/l Bacto-Trypton; 5 g/l Bacto-Yeastextract; 8 g/l NaCl; 1 g/l Glucose. pH 7.2. Before using 100 mg/l ampicillin or canamycin was added.
Luria-Bertani-Agar plates (LB-Plates)	15 g agar was dissolved in 1 l LB-medium and autoclaved. After cooling to 55°C, 1 mg/ml ampicillin was added.
SOC-Medium	20 g/l Bacto-Trypton, 5 g/l Yeast extract, 2.5 mM NaCl, 10 mM MgCl <sub>2</sub> , 10 mM, MgSO <sub>4</sub> , 20 mM Glucose.

#### 2.3.2 Media for cell culture

293T	DMEM	Dulbecco's modified Eagle Medium (Gibco, Darmstadt, Germany) supplemented with 10% (v/v) heat inactivated FCS, the antibiotics penicillin [120 µg/ml] and streptomycin [120 µg/ml], MEM sodium pyruvate and 350 µg/ml L-glutamine.
CemM7 Jurkat-LTRG R5	RPMI	RPMI-1640 (Gibco, Darmstadt, Germany) supplemented with 10% (v/v) heat inactivated FCS, the antibiotics penicillin [120 µg/ml] and streptomycin [120 µg/ml], MEM sodium pyruvate and 350 µg/ml L-glutamine.
MDM	MDM-medium	RPMI-1640 (Gibco, Darmstadt, Germany) supplemented with 4% (v/v) human AB-serum, the antibiotics penicillin [120 µg/ml] and streptomycin [120 µg/ml], MEM non-essential amino acids solution 10 mM, MEM sodium pyruvate, MEM vitamins and 350 µg/ml L-glutamine.

## 2.4 Nucleic acids

### 2.4.1 Oligonucleotides for site-directed mutagenesis

Following oligonucleotides were ordered from Biomers (Ulm, Germany); the most important cutting sites are italic:

**Name**                      **Sequence (5'-3' direction)**

Gag-iCFP_MluI	TCGACGCGTATGGTGAGCAAGGGCGAG
Gag-iCFP_XbaI	ACGTCTAGACTTGTACAGCTCGTCCAT
GAG_NheI	CCGCTAGCATGGGTGCGAGAGCGTTCGGTATTAAGCGGG
GAG_AgeI	CGACCGGTGCACCTGCTCCTTGTGACGAGGGGTGCTGC
CD81_XhoI	ATCTCGAGCTATGGGAGTGGAGGGCTGCAC
CD81_EcoRI	CTGAATTCTTAAACTCATTGTCAATGTCC
TfR_EcoRI	CAGAAATTCATTATCAGTACACGGAGCTGTTC
TfR_XhoI	CGCTCGAGCTATGATGGATCAAGCTAG
CD9_EcoRI	CAGAAATTCCTAGACCATCTCGCGGTTCC
CD9_XhoI	ATCTCGAGCTATGCCGGTCAAAGGAGGCAC
CD53_XhoI	ATCTCGAGCTATGGGCATGAGTAGCTTGAA
CD53_EcoRI	CAGAAATTCATAGCCCTATGGTCTGGC

### 2.4.2 Plasmids

Name	Description	Reference
HIV-1 pUC-NL4-3 Gag-iGFP	pUC vector, that has the HIV-1 NL43 provirus. There a GFP tag flanked by two protease cleavage sites was inserted between p17 MA and p24 CA	Hübner et al., 2007
pBR-NL4-3 92th014.12 (= "HIV-1 WT")	pBr322 vector, that has the HIV-1 NL43 provirus with the V3-loop 92th014.12	Papkalla et al., 2002
pBR-NL4-3 IRES-eGFP	pBr322 vector, that has the HIV-1 NL43 provirus with a eGFP under the control of an IRES	Schindler et al., 2003
pBr-NL4-3 env*	pBr322 vector, that has the HIV-1 NL43 provirus which does not express the Gp160 Env protein	Wildum et al., 2006
pEYFP-C1/N1	Clontech YFP expression vectors	Banning et al., 2010
pECFP-C1/N1	Clontech CFP expression vectors	Banning et al., 2010
pEYFP-MEM	A highly membrane localized protein (through palmitoylation) tagged with YFP	Banning et al., 2010
pEYFP-CD4	CD4 tagged with YFP	Banning et al., 2010
pEYFP-CFP	FRET positive control, YFP tagged CFP	Banning et al., 2010
pHIT-G	Expressionvector for the glycoprotein of <i>Vesicular Stomatitis Virus</i> (VSV-G)	Fouchier et al., 1997

### 2.4.3 DNA ladder

1-kb-ladder    Invitrogen (Karlsruhe, Germany)

### 2.4.4 Nucleotides for Polymerase-chain-reaction

dNTPs for PCR    Invitrogen (Karlsruhe, Germany)



## 2.5 Enzymes

### 2.5.1 Restriction endonucleases

Restriction endonucleases were ordered from New England Biolabs GmbH (Frankfurt, Germany) or Fermentas GmbH (St. Leon-Rot, Germany) and used with the buffer systems approved by the manufacturer.

### 2.5.2 Other enzymes

Name	Manufacturer
0.05% EDTA-Trypsin	Invitrogen/Gibco (Karlsruhe, Germany)
Alkalic Phosphatase	Roche (Mannheim, Germany)
T4-DNA-Ligase	Promega GmbH (Mannheim, Germany)
Dream Taq™ DNA Polymerase	Fermentas GmbH (St. Leon-Rot, Germany)
Pfu DNA Polymerase	Fermentas GmbH (St. Leon-Rot, Germany)

## 2.6 Antibodies

### 2.6.1 Primary antibodies

Antigen	Clone	Origin	Dilution	Manufacturer/Reference
HIV-1 Gag	KC57-RD1	Mouse	1:100	Beckman-Coulter (Krefeld, Germany)
HIV-1 Gp120	2G12	Human	1:100	Polymun Scientific (Klosterneuburg, Austria)
HIV-1 Gp120	VRC01	Human	1:50	Wu et al., 2010
HIV-1 Gp120	VRC03	Human	1:50	Wu et al., 2010
Human CD81	1.3.3.2.2	Mouse	1:100	Ancell (Bayport, USA)
Human TfR	MEM-75	Mouse	1:100	Abcam (Cambridge, UK)

### 2.6.2 Secondary antibodies

Name	Dilution	Manufacturer
Alexa Fluor® 633 goat anti-human IgG (H+L)	1:500	Invitrogen (Darmstadt, Germany)
Alexa Fluor® 555 goat anti-mouse IgG (H+L)	1:500	Invitrogen (Darmstadt, Germany)

## 2.7 Reagents

### 2.7.1 Chemicals

Name	Manufacturer
Agar	Carl Roth® GmbH & Co.KG (Karlsruhe, Germany)
Agarose	Carl Roth® GmbH & Co.KG (Karlsruhe, Germany)
Ampicillin	Ratiopharm GmbH (Ulm, Germany)
Bacto-Trypton	BD Biosciences Pharmingen (San Diego, USA)
Ethylen-Diamin-Tetraacetat (EDTA)	Carl Roth® GmbH & Co.KG (Karlsruhe, Germany)
Ethanol	Carl Roth® GmbH & Co.KG (Karlsruhe, Germany)
Ethidiumbromid	Carl Roth® GmbH & Co.KG (Karlsruhe, Germany)
Glucose	Merck KGaA (Darmstadt, Germany)
Yeast extract	BD Biosciences Pharmingen (San Diego, USA)
HPLC water	AppliChem (Darmstadt, Germany)
Isopropanol	Carl Roth® GmbH & Co.KG (Karlsruhe, Germany)
Kanamycin	Ratiopharm GmbH (Ulm, Germany)

MgCl <sub>2</sub>	Carl Roth® GmbH & Co.KG (Karlsruhe, Germany)
NaCl	Carl Roth® GmbH & Co.KG (Karlsruhe, Germany)
NaOH	Carl Roth® GmbH & Co.KG (Karlsruhe, Germany)
Paraformaldehyde (PFA)	Carl Roth® GmbH & Co.KG (Karlsruhe, Germany)
Phosphate Buffered Saline (PBS)	PAA (Cölbe, Germany)
DEPC (Diethylpyrocarbonat)	Carl Roth® GmbH & Co.KG (Karlsruhe, Germany)
Sodium acetat	Promega GmbH (Mannheim, Germany)
Sucrose, Ultrapure Bioreagent	Thomas scientific (Swedesboro, Germany)
Elisa wash solution	KPL (Gaithersburg, USA)
Sure blue PeroxidaseSubstrat	KPL (Gaithersburg, USA)
DMSO	Merck KGaA (Darmstadt, Germany)
L-glutamine	PAA Laboratories GmbH (Cölbe, Germany)
MEM non essential amino acids	PAA Laboratories GmbH (Cölbe, Germany)
Penicillin/Streptomycin	PAA Laboratories GmbH (Cölbe, Germany)
Fetal Craft's serum (FCS)	Gibco (Darmstadt, Germany)
MEM sodium pyruvate	Gibco (Darmstadt, Germany)
Human AB-serum	Sigma (München, Germany)
MEM Vitamins	Biochrom (Berlin, Germany)
Normal Goat Serum	Gibco (Darmstadt, Germany)
Normal Mouse Serum	Sigma (München, Germany)
Triton X-100	Sigma (München, Germany)

### 2.7.2 Reagent systems (Kits)

Name	Manufacturer
Resuspension buffer (P1)	Qiagen (Hilden, Germany)
Lysis buffer (P2)	Qiagen (Hilden, Germany)
Neutralization buffer (P3)	Qiagen (Hilden, Germany)
PureYield™ Plasmid Midiprep	Promega GmbH (Mannheim, Germany)
Ultra Clean™ 15 DNA Purification Kit	Dianova GmbH (Hamburg, Germany)
TA Cloning® Kit	Invitrogen/Gibco (Karlsruhe, Germany)
Takara DNA Ligation kit	Böhringer Ingelheim (Heidelberg, Germany)
Human Macrophage Nucleofector Kit	Lonza Cologne GmbH (Basel, Switzerland)
HIV-1 P24 Antigen Capture Assay Kit	AIDS Repository (Frederick, USA)
Calcium Phosphate Transfection Kits	Clontech (Saint-Germain-en-Laye, France)

### 2.8 Buffer and solutions

Name	Compounds
FACS-Buffer	1% FCS; 1 mM EDTA in PBS
Mowiol	0.2 M Tris-HCl, pH 8.5; 12% (w/v) Mowiol 4-88; 30% (w/v) Glyzerin
DEPC-H <sub>2</sub> O	0.5% (v/v) DEPC was added to steril H <sub>2</sub> O, incubated over night and autoclaved at the end

## 2.9 Laboratory equipment

<b>Name</b>	<b>Manufacturer</b>
DNA Gel electrophoresis system	Bio-Rad Laboratories (Hercules, USA)
Eppendorf centrifuge 5417 R	Eppendorf (Hamburg, Germany)
Eppendorf centrifuge 5810 R	Eppendorf (Hamburg, Germany)
FACSCantoII™	B&D, Becton Dickinson, Immunocytometry Systems, (San José, USA)
GeneAmp® PCR System 9700	AB Applied Biosystems (Darmstadt, Germany)
HERAsafe® Inkubator	Thermo Fisher Scientific GmbH (Hanau, Germany)
HERAsafe® laminar flow	Thermo Fisher Scientific GmbH (Hanau, Germany)
Infinite® M200	Tecan Group Ltd. (Männedorf, Switzerland)
Nanodrop ND-1000	PEQLAB Biotechnology GmbH (Erlangen, Germany)
Nikon Eclipse Ti	Nikon (Tokyo, Japan)
Nikon Eclipse TS100	Nikon (Tokyo, Japan)
Nucleofector® II Device	Lonza Cologne GmbH (Basel, Switzerland)
Odyssey Imaging System Li-Cor	Biotechnology GmbH (Bad Homburg)
Philips CM 120 TEM	Philips (Eindhoven, Netherlands)
Shaker Innova® 43 Shaker	New Brunswick (Nürtingen, Germany)
SW40 Ti Rotor Package, Swing Bucket	Beckman Coulter (Krefeld, Germany)
Thermoblock	Eppendorf (Hamburg, Germany)
Ultracentrifuge L8-55M	Beckman Coulter (Krefeld, Germany)
UV-Transilluminator GelDoc 2000	Hartenstein (Würzburg, Germany)
Vortex-Genie 2	Scientific Industries (New York, USA)
Zeiss 510 Meta	Carl Zeiss (Jena, Germany)

## 3 Methods

### 3.1 Molecular biological methods

#### 3.1.1 DNA-standard methods

The following methods were performed as described in Maniatis et al., 1989:

- Plasmid-DNA-Isolation post alkaline bacteria lysis
- Ethanol- and Isopropanol precipitation of DNA
- Dephosphorylation of DNA 5' ends by alkaline phosphatase
- Digestion of DNA using restriction endonucleases
- Ligation of DNA-Fragments using T4-DNA-Ligase
- Separation of nucleic acids by gel electrophoresis

#### 3.1.2 Transformation of *E. coli* One Shot® Top10

After thawing *E.coli* on ice, 10 µl bacteria solution were mixed with 2.5 µl ligation mix and preincubated for 15 min on ice. Next, the heat shock was performed for 45 sec at 42°C. 150 µl SOC-media was added and bacteria were incubated at 37°C for 30 min. At the end, the bacteria solution was plated on LB-plates and incubated at 37°C over night. All used plasmids were grown on ampicillin positive plates except the pECFP/ pEYFP constructs that were grown on kanamycin positive plates.

#### 3.1.3 Isolation of plasmid-DNA

For isolation of plasmid DNA from bacteria, two methods were used. The first method called mini-preparation was used after cloning to detect positive clones.

The second method called midi-preparation was used to get high amounts of a correct construct as a plasmid DNA working stock.

DNA concentrations were measured using a nanodrop ND-1000 (PqLab)

##### 3.1.3.1 Mini preparation

5 ml overnight culture was centrifuged at 3200x g for 10 min. The pellet was resuspended in 300 µl Qiagen resuspension buffer (P1) and lysed with 300 µl Qiagen lysis buffer (P2) by inverting the tube. The lysis was stopped by addition of 300 µl Qiagen neutralization buffer (P3). The lysate was centrifuged at 20 000x g for 25 min and supernatant was precipitated with 500 µl Isopropanol for 10 min and centrifuged at 20 000x g for 30 min. Afterwards, the pellet was washed with 70% ethanol by centrifugation at 20 000x g for 5 min. At the end, the pellet was dried and dissolved in 50 µl ddH<sub>2</sub>O.

### 3.1.3.2 Midi preparation

To get high amounts of plasmid DNA, a so called midi preparation starting with 500 ml over night culture was performed using the PureYield™ Plasmid Midiprep kit from Promega. All preparation steps were performed as described in the instruction manual.

### 3.1.4 Isolation of DNA from agarose gels

To isolate the correct DNA fragment, for example after restriction endonuclease treatment, DNA fragments were separated by their length at a 1% ethidium bromide yielding agarose gel by electrophoresis. At 366 nm UV-light DNA bands were made visible and cut out. DNA was isolated by the Ultra Clean™ 15 DNA Purification Kit from Bionova.

### 3.1.5 Polymerase chain reaction (PCR)

The polymerase chain reaction is a standard molecular method and explained for example in Saiki et al., 1988. In this work the following program was used to amplify genes using a Gene Amp PCR System 9700 von Applied Biosystems:

<b>cycles</b>	<b>temperature</b>	<b>duration</b>	
1	96°C	5 min	Initial Denaturation
	96°C	45 sec	Denaturation
35	50°C	45 sec	Hybridization of oligonucleotides
	72°C	2 min	Elongation
1	72°C	8 min	Final Elongation
	4°C	∞	

For reaction mix, 5 µl 10x DreamTaq Reaction Buffer, 75 pmol 5'- and 3' primer, 10 mmol dNTP mix, 0.25 µl DreamTaq and 40 µl ddH<sub>2</sub>O were used. Primers were ordered by biomers.net GmbH (Ulm). The PCR products were separated by 1% agarose gel electrophoresis and isolated as described above (M&M 3.1.4).

### 3.1.6 Sequencing

Sequencing of plasmid DNA isolated by mini preparation was commercially done by MWG-Biotech AG or SeqLab using their protocols.

### 3.1.7 Generation of HIV-1 provirus and expression vectors

PCR products and plasmids were digested with 0.25 µl of used restriction endonucleases for 25 min at 37°C. Vector plasmids are additionally treated with 0.5 µl alkaline phosphatase. After digestion, DNA

fragments were separated by 1% agarose gel and isolated as described above (M&M 3.1.4). The isolated fragments were ligated at a ratio of vector vs. insert of 1:4 for two hours at 16°C using the Takara DNA Ligation kit from Böhlinger Ingelheim. At the end the ligation mix was transformed into *E.coli* as described above (M&M 3.1.2).

### **3.1.7.1 Generation of pBR-NL4-3-V3 92th014.12\_Gag-iGFP and -iCFP constructs**

To generate a R5 tropic construct of the described pUC-NL4-3 Gag-iGFP (Hübner et al., 2007) the Gag-iGFP cassette was excised by restriction endonucleases BssHI and AgeI and ligated into the pBr-NL4-3 backbone (Carl et al., 2000).

Then the *env* gene harbouring the R5 tropic V3 loop of pBR-NL4-3 92th014.12 (Papkalla et al., 2002) was introduced through NheI and StuI restriction enzymes and ligated into the new construct.

To construct a CFP tagged version, CFP was amplified with the primers GagiCFP\_MluI and GagiCFP\_XbaI and ligated into pUC-NL4-3 Gag-iGFP. For the R5 tropic construct the same strategy was used as described above.

For TIRF analysis an uninfecious *env*-defective pBR-NL4-3 Gag-iGFP was designed by replacing the *env* gene (AgeI and HpaI) with that of pBr-NL4-3 *env*\* (Wildum et al., 2006) containing a premature stop codon and a frame-shift in *env*.

### **3.1.7.2 Generation of pBR-NL4-3-V3 92th014.12\_IRES-eGFP (R5 tropic HIV-1 GFP)**

For the generation of a macrophage tropic construct of pBR-NL4-3 IRES-eGFP (Schindler et al., 2003), the same strategy was used as described above (M&M 3.1.7.1.).

### **3.1.7.3 Generation of constructs for FACS-based FRET measurements**

Controls and cloning strategy of FACS-based FRET constructs was described in Banning et al., 2010. To generate the new N-terminal tagged constructs pEYFP-CD81, pEYFP-CD9, pEYFP-CD53 and pEYFP-TfR, genes were amplified from a Jurkat cDNA library by PCR using the primer listed in M&M 2.4.1, cut by XhoI and EcoRI and ligated into pEYFP-C1. CD82 was ordered from MWG, cut by XhoI and EcoRI and ligated into pEYFP-C1. To generate C-terminal pECFP-Gag HIV-1 *gag* was amplified with the primers GAG\_NheI and GAG\_AgeI from pBR-NL4-3 92th014.12, cut by NheI and AgeI and ligated into pECFP-N1.

## **3.2 Cell biological methods**

### **3.2.1 Cultivation of adherent and suspension cell**

The adherent cell line 293T was cultivated at 37°C and 5% CO<sub>2</sub> in cell culture flasks in DMEM supplemented with 10% fetal calf serum (FCS; Invitrogen), the antibiotics penicillin and streptomycin, and 1% L-glutamin (PAA). Cells were subcultivated twice a week at a ratio of 1:20.

Macrophages were cultivated at 37°C and 5% CO<sub>2</sub> in MDM medium (see M&M 2.3.2). Until the cells were used for experiments, they were grown in 100x 15 mm petri dishes with vent (Greiner bio-one) making them prone for Trypsin/ EDTA (0.05%) detachment.

Suspension cell lines Jurkat-LTRG R5 and CemM7 were also cultivated in cell culture flasks at 37°C and 5% CO<sub>2</sub>. These cell lines were maintained in RPMI with the supplements 10% fetal calf serum (FCS; Invitrogen), the antibiotics penicillin and streptomycin, and 1% L-glutamin (PAA) and were subcultivated twice a week in ratio 1:10.

### **3.2.2 Isolation of mononuclear cells from peripheral blood**

Monocyte derived macrophages (MDM) were derived from Buffy Coats (Concentrated Lymphocytes from 500 ml human blood) from the blood donation center at the UKE Hamburg. Only CMV negative Buffy Coats were used.

A Buffy Coat was diluted with PBS at a ratio 1:2 and peripheral blood mononuclear cells (PBMCs) were isolated by Ficoll (Biochrom) gradient centrifugation: 800x g for 35 min with lowest acceleration and without break. The central PBMC containing fraction was washed twice with PBS and PBMC were seeded in 100x 15 mm petri dishes with vent (Greiner bio-one) at a density of 1.5 Mio PBMC per ml in MDM medium. During cultivation for 4 days monocytes adhered at the bottom of the plates. After this period the suspension cells (mainly lymphocytes), were washed out with PBS. The adherent monocytes were cultivated for 3 additional days in MDM medium allowing differentiation to macrophages.

### **3.2.3 Generation of virus stocks by calcium phosphate transfection of 293T cells**

For the generation of virus stocks, 293T cells were transfected with provirus DNA-plasmids using the Calcium Phosphate Transfection Kit (Clontech). 12 hours before transfection 300 000 cells were seeded in 6-wells. When cells reached a confluence of 50-70% they could be used for transfection: 5 µg plasmid DNA was mixed with 13 µl 2M CaCl<sub>2</sub> and diluted with 80 µl ddH<sub>2</sub>O. This mixture was added drop wise to 100 µl 2x HBS and vortexed. After 5 min of incubation at room temperature the solution was pipetted drop wise into the medium covering the cells. Medium was change after 8

hours of incubation. Two days post transfection the virus containing supernatant was centrifuged at 1800x g for 5 min.

Additionally to the proviral plasmid DNA 0.5 µg VSV-G was used for the generation of env defective virus stocks that were only competent for a single round of infection.

### **3.2.4 HIV-1 p24 capsid antigen-ELISA**

To quantify the amount of p24 capsid in virus stocks or cell supernatants, virus was lysed with Triton X-100 (Sigma) at 4°C for 12 hours. HIV-1 P24 Antigen Capture Assay Kit (AIDS Repository) was used to measure the amount of the capsid protein p24 that was bound to a monoclonal mouse antibody. Unbound material was removed by several washing steps. First a polyclonal rabbit antibody was added to bind p24 capsid. After washing, the bound antibody was incubated with a goat anti rabbit antibody coupled to a peroxidase. The excess antibody was washed away. Addition of Sure blue Peroxidase Substrat (KPL) lead to a color change of the solution, indicating coupled antibodies to p24. This color change could be detected at an Infinite® M200 (Tecan) at 450 nm and 650 nm.

### **3.2.5 Infectivity assay**

Jurkat-LTRG R5 cells were infected with pBR-NL4-3-V3 92th014.12\_Gag-iGFP or pBr-NL4-3-V3 92th014.12 for infectivity assay with the indicated amounts of p24. 3 days post infection infected cells expressing GFP were fixed with 2% PFA and quantified by standard FACS measurement.

### **3.2.6 Infection of monocyte derived macrophages**

MDM were seeded 12 hours before infection at a density of 100 000 cells per ml in different well plates (Grainer) or in 35 mm dishes with or without grid (Ibidi) for microscopy. For infection the medium was removed and virus stock (50 ng p24 per 50 000 cells, if not indicated otherwise) was put onto the cells and cells were incubated for 8 hours at 37°C. Afterwards virus-containing medium was removed, cells were washed with PBS and new medium was added. Cells were cultivated again for different days, depending on the experimental settings.

### **3.2.7 Co-cultivation experiments**

For co-cultivation experiments MDM were seeded in 24 wells (Grainer) and infected with pBR-NL4-3-V3 92th014.12\_IRES-eGFP with 20 ng p24 as described above (M&M 3.2.6). 6 days post infection cells were washed with PBS to remove free virus. Then MDM were incubated with 20 µg per ml anti-TfR or anti-Gp120 2G12 antibodies for one hour at 37°C. After washing out excess antibody, 100 000 CemM7 T-cells per well were added to the MDM and cocultured for 10 hours. Afterwards CemM7 T-cells were harvested by cold 5 mM EDTA/PBS and recultured in 500 µl RPMI for 3-4 days. Infected cells expressing GFP were fixed with 2% PFA and quantified by standard FACS measurement.



### 3.2.8 FACS-based FRET assay

Method and gating strategy of FACS-based FRET assay was described in Banning et al., 2010. For this assay 300 000 293T cells were seeded in 6 well plates 12 hours before transfection. In this assay a CFP tagged gene of interest and an YFP tagged gene of interest is co-transfected using Calcium Phosphate Transfection Kits (Clontech) as described above (M&M 3.2.3). If the distance between the two proteins is less than 10 nm, there is energy transfer from the excited CFP to the YFP. So, by exciting CFP and measuring the emission of YFP a possible very close colocalization or interaction could be detected. Cells were harvested one day post transfection, washed with FACS-Buffer and FRET could be measured in a FACS Cantoll (BD Bioscience).

	Extinction measured at	Emission measured with
CFP	405 nm	standard 450/40 filter
YFP	488 nm	529/24 filter (Semrock)
FRET	405 nm	529/24 filter (Semrock)

### 3.2.9 Nucleofection of monocyte derived macrophages

Plasmid DNA was electroporated into MDM using Amaxxa Human Macrophage Nucleofector Kit (Lonza) following protocol instructions provided by the manufacturer and using the program Y-10. 24 hours post electroporation, cells were fixed with 2% PFA and analyzed by confocal microscopy.

## 3.3 Microscopy

### 3.3.1 Live-cell microscopy

The generation of an infectious GFP tagged macrophage tropic HIV-1 construct allowed visualizing HIV-1 particles and Gag accumulations in living primary macrophages. A fully motorized Nikon Ti-Eclipse microscope was used for live cell imaging. The microscope was equipped with the hardware based perfect focus system and the Nikon DS-Qi1 high speed monochrome digital camera. A CFI Apochromat 60x TIRF objective (NA 1.49) was used in most of the cases, only imaging of the infection process was done with a 40x Plan Fluor objective (Nikon). 200 000 MDM were seeded in a  $\mu$ -Dish (35 mm high, Ibidi) and infected as described above (M&M 3.2.6). During imaging cells were kept in a microscope desk mounted TokaiHit incubation chamber at 37°C and 5% CO<sub>2</sub>, allowing to image infected MDM over long periods of several hours and even days.

### 3.3.2 TIRF microscopy

Total internal reflection fluorescence (TIRF) microscopy was used to visualize possible HIV-1 budding events at the plasma membrane of infected macrophages. The technique is described in Results 4.4.

100 000 MDM were seeded in 35 mm glass bottom culture dishes for TIRF (MaTek) and infected as described above (M&M 3.2.6). 3 days later, 200 000 293T cells were seeded into a 6-well and were infected in the same way as described for the MDM. One day post infection 293T cells were detached and put to the infected MDM (5 dpi). 5 hours later 293T cells have been adhered and were imaged by a fully motorized Nikon Ti-Eclipse microscope with the hardware based perfect focus system and the Nikon DS-Qi1 high speed monochrome digital camera using the CFI Apochromat 60x TIRF objective (NA 1.49).

TIRF imaging was supported by Dr. Rudolf Reimer from the research group for electron microscopy at the Heinrich-Pette-Institute.

### **3.3.3 Confocal fluorescence microscopy and staining**

200 000 MDM were seeded in 12 well plates with an added cover slip and infected with the HIV-1 GC as described above (M&M 3.2.6). 6 dpi cover slips with cells that should be permeabilized were washed with PBS, fixed with 2% PFA for 30 min at 4°C and permeabilized with 1% Saponin/ PBS for 10 min at room temperature. After blocking with 10% FCS/ PBS for 20 min at room temperature, cells were stained with primary antibodies for 30 min at room temperature. Other cells were washed with PBS but neither fixed nor permeabilized before staining with primary antibodies for 60 min at 4°C or at 37°C, then washed with PBS, fixed with 2% PFA, permeabilized with 1% Saponin/ PBS and blocked with 10% FCS/ PBS for 20 min at room temperature. After washing with PBS, all cells were stained with secondary antibodies for 20 min at room temperature. Finally, the cells were mounted on microscope slides using mowiol mounting solution (2.4 g polyvinylalcohol, 6 g Glycerin, 18 ml PBS) and imaged with a Zeiss LSM510 Meta.

### **3.3.4 Correlative transmission electron microscopy**

The advantage of infectious GFP tagged HIV-1 could be used to circumvent the problem that only 2-10% of MDM get infected. Correlative EM was used to compare a specific intracellular Gag accumulation between fluorescence microscopy and EM. 100 000 MDM were seeded in a  $\mu$ -Dish with imprinted relocalization grid (35 mm high with Grid-500, Ibidi) and infected as described above (M&M 3.2.7). 7 dpi DIC and epifluorescent images were made using live cell microscopy (see M&M 3.3.1) and the correct location at the grid was noted. Then the cells were fixed with 2.5% glutaraldehyde (GA) in PBS for 30 minutes at room temperature, washed with PBS, incubated with 1% OsO<sub>4</sub> in PBS for 30 min, washed with ddH<sub>2</sub>O and 1% uranyl acetate in water. Ethanol was used to gradually dehydrate the samples before cells were embedded with Epon resin for sectioning. The exact cell of interest was found by using the relocalization grid and 50 nm ultra thin serial cuts were made parallel to the bottom of the dish using an Ultracut Microtome (Reichert Jung). The cuts were

contrasted with 2% uranyl acetate for 7 min at room temperature and lead citrate for 3 min at room temperature. EM cuts were imaged using a FEI Eagle 4k HS CCD camera attached to a FEI Technai G<sup>2</sup> 20 Twin transmission electron microscope (FEI) at 80 kV.

All steps post GA fixation were done by Carola Schneider from the research group for electron microscopy at the Heinrich-Pette-Institute.

### **3.4 Imaging analysis and software**

Analysis of confocal microscopy images and 3D reconstruction of EM images were performed using Bitplane Imaris Software (V6.4.2.). Live cell images were analyzed with Nikon Elements AR V3.1 software and 2D real time deconvolution or 3D Huygens based deconvolution plug-ins or the AutoQuantX2 (MediaCybernetics) software. Both deconvolution softwares showed the same results. The freely available ImageJ V1.4.2 and VirtualDub V1.9.8 software packages were used to generate and compress movies and GraphPad Prism V5 software package was used for statistical analyses. In general, images were never modified apart from enhancing contrast and/ or brightness.

## 4 Results

In T-cells and most cell lines HIV-1 assembles and buds at the plasma membrane whereas in macrophages HIV-1 particles as well as budding events can be found at membranes that seem to be intracellular (Bieniasz, 2009; Gendelman et al., 1988; Ono, 2009; Orenstein et al., 1988). Most of these so called virus containing compartments (VCC) are found by electron microscopy (EM). Although EM is a well suited tool to study the subcellular organization of virus infected cells, it fails to give answers about the origin and fate of these structures (Bennett et al., 2009). To visualize Gag production and assembly sites in living primary macrophages a GFP tagged macrophage tropic HIV-1 construct that replicates in macrophages was generated, characterized and used during this thesis.

### 4.1 Generation and characterization of a macrophage tropic HIV-1 with an internal GFP-tag in the HIV-1 Gag polyprotein

Most of the GFP tagged HIV-1 constructs that were described during the last decade did not replicate in primary cells and cell lines (Jouvenet et al., 2006; Muller et al., 2004). This situation changed when Ben Chen's group introduced HIV-1 with a GFP tag inside the Gag polyprotein. To retain infectivity the GFP cassette was introduced between the p17 matrix and the p24 capsid protein flanked by HIV-1 protease cleavage sites (Figure 6.1) (Hübner et al., 2007). During assembly the GFP tagged Gag polyprotein is incorporated into the immature virion. When the virion matures the viral protease cleaves the Gag polyprotein and GFP, staying within the virion. Using this T-cell tropic HIV-1 construct it was possible to image cell-to-cell transfer between T-cells. (Hübner et al., 2009)

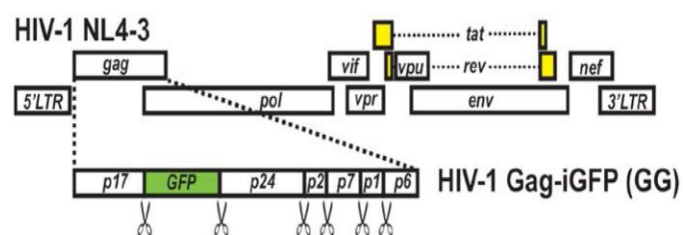


**Figure 6.1 Schematic genome organization of HIV-1 Gag-iGFP (HIV-1 GG).**

GFP is inserted between p17 MA and p24 CA of the Gag precursor and flanked by two protease cleavage sites leading to the release of GFP during particle maturation.

(modified from Hübner et al., 2007)

#### 4.1.1 Characterization of pBR-NL4-3-V3 92th014.12\_Gag-iGFP (HIV-1 GG)

Available GFP expressing HIV-1 constructs cannot be used to infect macrophages because of their X4-tropism and low infectivity (Hübner et al., 2009). Therefore, a macrophage tropic variant was generated to analyze assembly and budding in macrophages (see M&M 3.1.7.1).

HIV-1 GG should allow differentiation of free Gag and assembly sites with faint GFP expression representing free Gag whereas larger GFP accumulations might represent Gag assembly or budded virions. To verify that GFP resembles HIV-1 Gag, infected macrophages were permeabilized and stained with antibodies against Gag. The exact colocalization of GFP and Gag demonstrates that in HIV-1 GG infected macrophages GFP is a marker for Gag. Furthermore faint GFP/ free Gag was distributed in the cytoplasm and at the plasma membrane, whereas large GFP accumulations were found inside the macrophage (Figure 6.2).

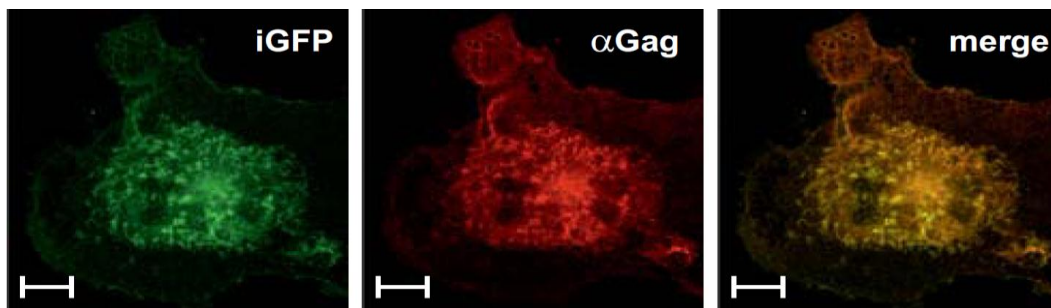


**Figure 6.2 GFP expression resembles Gag distribution in HIV-1 GG-infected macrophages.**

Four days postinfection MDM were stained with mouse anti-Gag antibodies ( $\alpha$ Gag) and subcellular localization of GFP as well as Gag expression were analyzed by confocal microscopy. The scale bar indicates 10  $\mu$ m.

Next, the localization of Gag assembly sites in different cell types was determined. By cotransfecting the HIV-1 GG proviral DNA together with a plasmid encoding for the vesicular stomatitis virus glycoprotein (VSV-G) viral particles incorporate VSV-G into their membranes. This process is called pseudotyping and allows HIV-1 to infect cells independent of CD4 or the chemokine coreceptor (Wildum et al., 2006). 293T cells, Jurkat T-cells and MDM were infected with pseudotyped HIV-1 GG and localization of Gag accumulations was detected. As expected, in 293T and Jurkat T-cells Gag was mainly localized at the plasma membrane, whereas macrophages accumulated Gag in areas which might be intracellular (Figure 6.3).

Next, infectivity and replication of HIV-1 GG for CCR5 positive CD4+ T-cells and macrophages was assessed. For this Jurkat-LTRG R5 cells, CD4+ T-cells that express the CCR5 coreceptor and GFP under control of the Tat promoter, were infected with different amounts of HIV-1 wild type or with HIV-1 GG. Two days later infectivity could be quantified by measuring GFP by FACS. Although the infection

rate of HIV-1 wild type was 2 to 3 fold higher, HIV-1 GG retained its ability to infect CCR5 positive cells in a dose dependent manner (Figure 6.4 A).

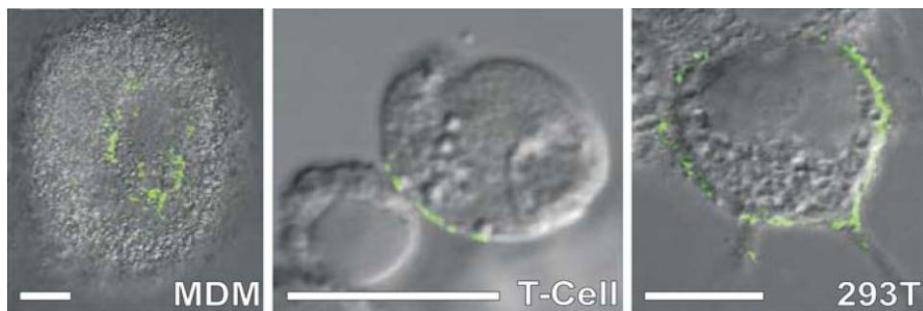


**Figure 6.3 Gag accumulations and sites of HIV-1 assembly in HIV-1 infected cells.**

MDM, primary T-cells or 293T cells were infected with VSV-G pseudotyped HIV-1 GG and subcellular localization of Gag/GFP expression was analyzed by confocal microscopy. Presented are overlays of Gag/GFP expression and DIC pictures. The scale bar indicates 10  $\mu$ m.

For replication analysis the supernatant of HIV-1 wild type or HIV-1 GG infected macrophages was collected every second day and p24 amounts were measured by ELISA. HIV-1 GG can infect and replicate in macrophages, although with approximately 50% loss of activity in comparison to untagged HIV-1. Nevertheless the replication peaked at day 4, with a kinetic that is comparable to wild type HIV-1 (Figure 6.4 B).

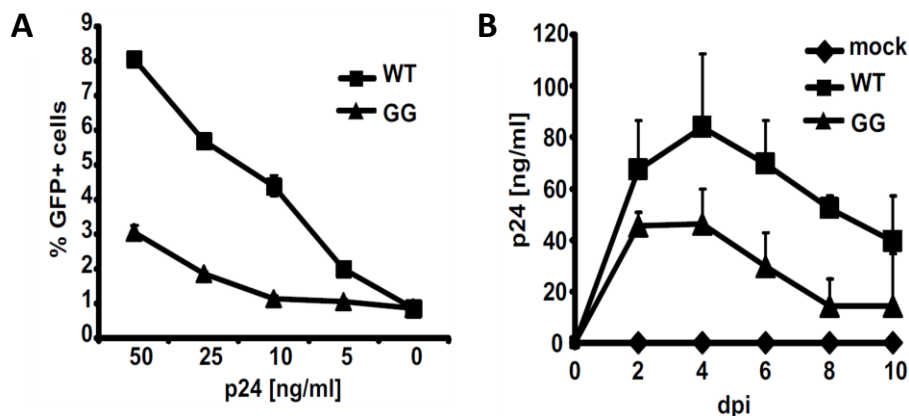


**Figure 6.4 Characterization of R5-tropic HIV-1 NL4-3 Gag-iGFP (HIV-1 GG).**

(A) Jurkat LTRG-R5 cells were infected with the indicated amounts (ng/ml) of p24 from either HIV-1 WT or HIV-1 GG, and the percentage of GFP-positive cells was determined 3 days later by flow cytometry. Means and standard deviations (SD) are derived from results from triplicate infections with two independent virus stocks.

(B) MDMs were infected with 50 ng of p24 from either HIV-1 WT or HIV-1 GG, and supernatants were taken in 2-day intervals measuring replication kinetics. P24 ELISA was used to determine virus in the supernatants. The graph shows mean values and SD from one experiment with MDM infected in triplicates with two independent virus stocks. Similar results were obtained with MDM from three other donors.

Characterization of R5-tropic GFP-tagged HIV-1 (HIV-1 GG) revealed that it is able to infect and replicate in macrophages. GFP expression is a marker for Gag localization and HIV-1 GG infected macrophages showed a similar pattern of Gag distribution in comparison to untagged HIV-1 (Benaroch et al., 2010). Thus, HIV-1 GG is a useful tool to investigate Gag trafficking, assembly and HIV-1 budding in primary macrophages in the context of infectious and replicating HIV-1.

#### 4.2 In HIV-1 infected macrophages Gag accumulates intracellular

In macrophages HIV-1 accumulates in VCCs, but the origin and fate of these structures is controversially discussed in the literature (Figure 6.2, 6.3; e.g. Benaroch et al., 2010; Welsch et al., 2007). In most cases VCCs were shown using electron microscopy which nicely allows to visualize structural features but is not conclusive in terms of dynamics since cells are fixed and embedded before analysis. By infecting living primary monocyted-derived-macrophages with HIV-1 GG the Gag distribution can be analyzed by live cell microscopy. Macrophages are differentiated cells and have a low expression rate for which reason they need some days to produce high amounts of progeny virions (Welsch et al., 2011). 4 days post infection with HIV-1 GG large accumulations of newly produced virus could be detected in fixed macrophages by confocal microscopy, whereas in the cytoplasm and at the plasma membrane only faint GFP signals could be detected (Figure 6.5).

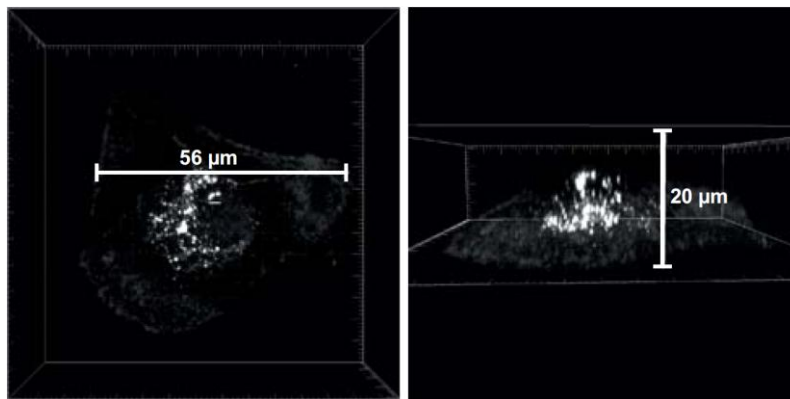


**Figure 6.5 Representative 3-D reconstruction of GFP/Gag distribution in HIV-1 GG-infected MDM.**

Z-stack of an infected macrophage was recorded 4 dpi by fluorescence confocal microscopy and reconstructed using Bitplane Imaris 6.4.2. Typically, Gag showed a pattern of intense accumulations near the central nucleus of the macrophage, in contrast to weak expression in the cytosol and at the plasma membrane.

Using live cell microscopy it is possible to track these accumulations for hours or even days. The image shown in Figure 6.6 is part of a time laps movie taken over a period of 4 days with one image per 15 minute interval to prevent photo bleaching of GFP. In line with the confocal analysis shown before (Figure 6.5) 4 days post infection faint Gag expression was detected all over the cytosol, but Gag accumulations were found in close vicinity to the perinuclear region of the macrophages. These larger accumulations stayed stable during the observation period (Figure 6.6). However, smaller Gag puncta were detected moving from the center of the cell to the periphery as well as from the periphery backwards to the center of the cell. Thus, Gag accumulations are relatively stable with constant trafficking of smaller Gag puncta. However, a distinct pattern of Gag movement could not be detected.

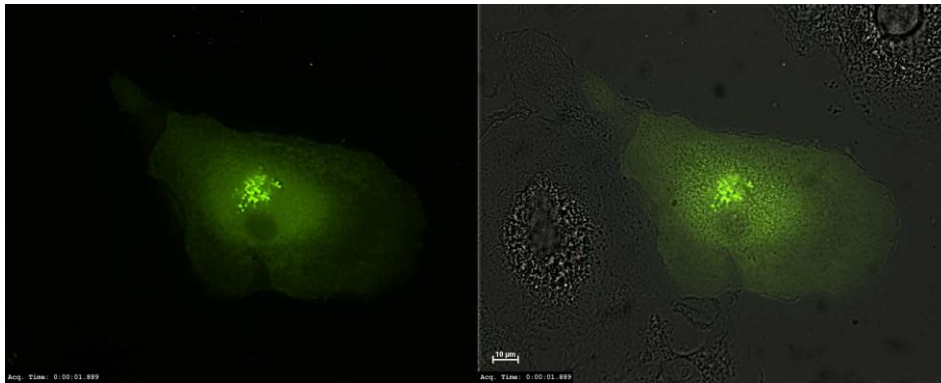


**Figure 6.6 Representative Live Cell Imaging of HIV-1 GG-infected MDM.**

Four days post infection, an infected macrophage was imaged every 15 min for 60 h. In this representative image big Gag accumulations are found in the perinuclear region while faint Gag is distributed over the whole cell.

The scale bar shows a distance of 10  $\mu\text{m}$ .

### 4.3 The temporal origin of macrophage internal Gag accumulations

In order to assess the formation of macrophage internal Gag accumulations time laps movies with HIV-1 GG infected macrophages were recorded. Macrophages were seeded in microscope dishes and imaged directly post infection in a microscope mounted incubation chamber. To prevent photo bleaching a temporal resolution of one image every 30 minutes was used (Figure 6.7). 30 to 36 hours post infection (hpi) faint GFP was expressed which was diffusely distributed in the cytosol. In this early phase no Gag accumulations could be detected; neither in intracellular compartments nor at the plasma membrane. 36 to 39.5 hpi first Gag accumulations appeared inside the macrophage near the center of the cell. During the next 33 hours of imaging this accumulation was enlarged and diverged into additional accumulations (Figure 6.7).



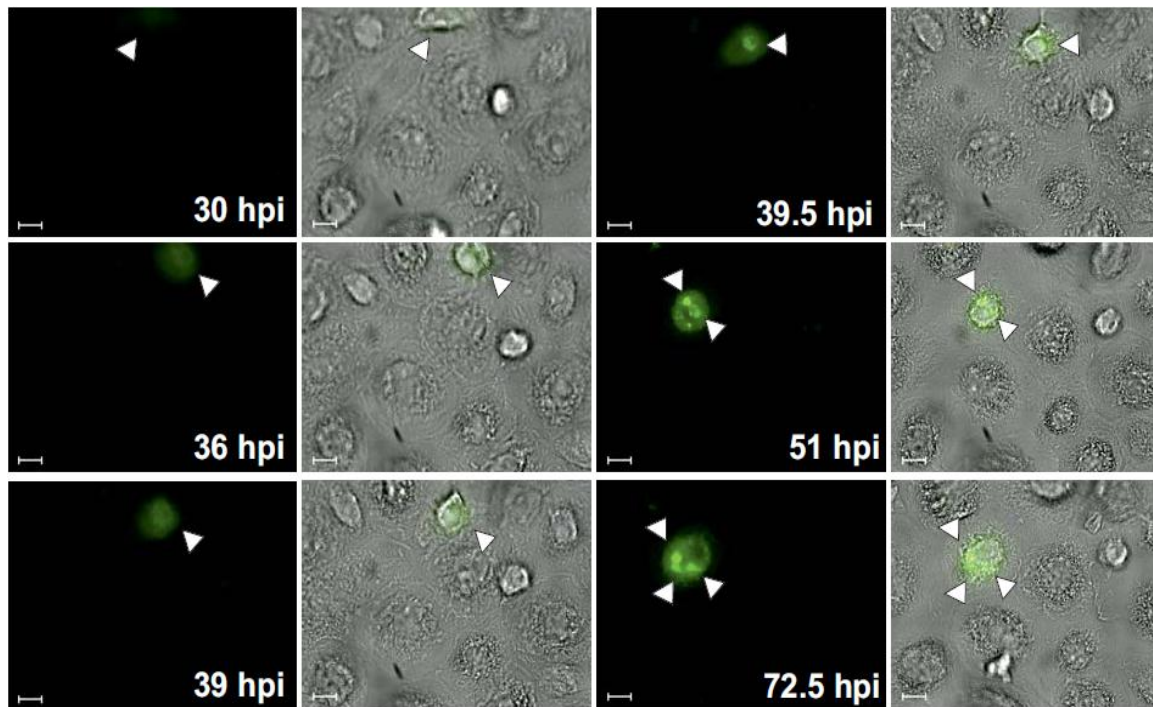


**Figure 6.7 Kinetics of Gag expression in HIV-1 GG-infected MDM.**

Macrophages were infected with HIV-1 GG and observed by time-lapse fluorescence microscopy for a period of 4 days. To prevent photo bleaching images were recorded every 30 min with a 40x Plan Fluor objective (Nikon). White arrowheads indicate areas of Gag expression and accumulation.

The scale bar shows a distance of 10  $\mu\text{m}$ .

Two-dimensional live cell imaging does not allow to assess the spatial localization of Gag. Therefore z-stacks of HIV-1 GG infected macrophages were recorded over time. In this setting the infected macrophage was imaged 4 dpi at a temporal resolution of one z-stack every 30 minutes over several hours. Figure 6.8 shows an example of a newly formed Gag accumulation appearing in the center of the cell (marked by the white square) within 30 minutes. During the next 2 hours this accumulation stayed stable and then suddenly moved towards the periphery of the cell and disappeared. Although some smaller Gag/GFP puncta could be detected in the periphery of the cell, the majority of Gag clustered inside the macrophage.

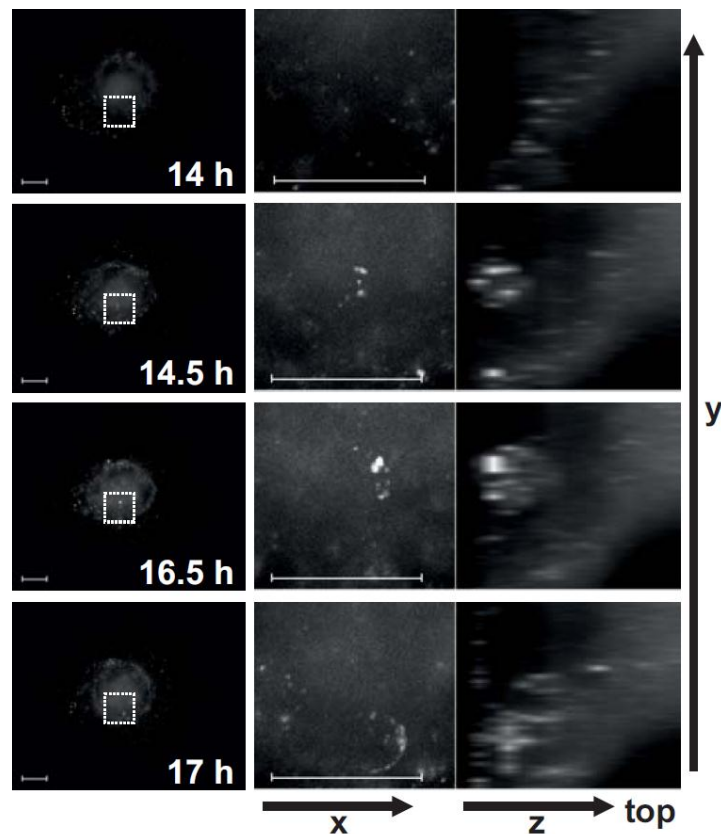


**Figure 6.8** Four-dimensional time lapse of an HIV-1 GG-infected macrophage.

Four days post infection, z-stacks of an HIV-1 GG-infected MDM were collected in 30 min intervals over a period of 24 h. Images depict a 3 h sequence in which a Gag accumulation (squared inlay) is generated intracellularly and disperses after a few hours. Z-stacks were deconvolved with a Huygens-based deconvolution algorithm (Nikon NIS Elements AR3.1). The scale bar shows a distance of 10  $\mu\text{m}$ .

#### 4.4 Absence of assembly sites at the plasma membrane of HIV-1 infected macrophages

Live cell microscopy suggests macrophage internal HIV-1 assembly and budding. Nevertheless, imaging techniques used thus far did not exclusively allow to investigate plasma membrane associated Gag trafficking. Thus, total internal reflection fluorescence (TIRF) microscopy was used to investigate the potential formation of assembly sites and HIV-1 budding at the plasma membrane of HIV-1 infected macrophages. Using TIRF microscopy the specimen is illuminated by a laser beam in a certain angle resulting in total reflection of the light at the borderline between sample and the glass bottom of the dish. This results in an evanescent field of light just exciting fluorophores 100-200nm above the plasma membrane, whereas chromophores deeper inside the cell stay unexcited (Figure 6.9). By this technique it was demonstrated that Gag assembly at the plasma membrane takes 6 to 8 minutes and the whole budding procedure is completed within up to 20 minutes (Ivanchenko et al., 2009).

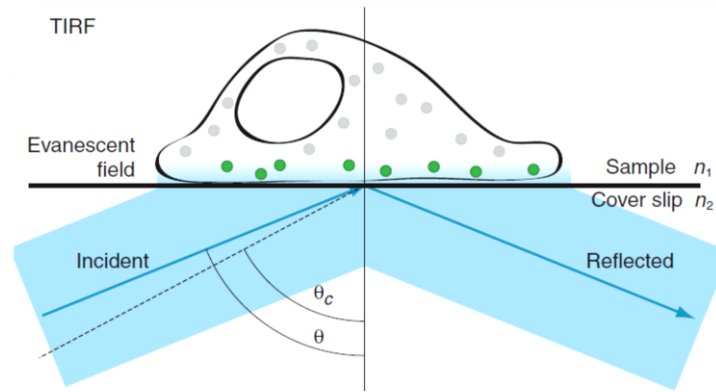


**Figure 6.9 Schematic presentation of Total internal reflection fluorescence technique.**

(Mattheyses et al., 2010)

As a control Gag trafficking at the plasma membrane of macrophages was compared to 293T cells, a cell type in which assembly of HIV-1 at the plasma membrane is well established. Infected 293T cells (1 dpi) that produce high amounts of new virions at the plasma membrane and infected macrophages (6 dpi) with typical intracellular Gag accumulations were cocultured. Both cell types were infected with env defective HIV-1 GG that was pseudotyped with VSV-G, because 293T cells do not express the primary HIV-1 receptor CD4. An area was chosen which allows to image infected 293T cells and an infected MDM (marked by the white circle) during the same acquisition step (Figure 6.10). As expected, macrophages displayed multiple intracellular Gag accumulations, whereas 293T cells showed Gag expression in the cytosol as well as at the plasma membrane (Figure 6.10 A).

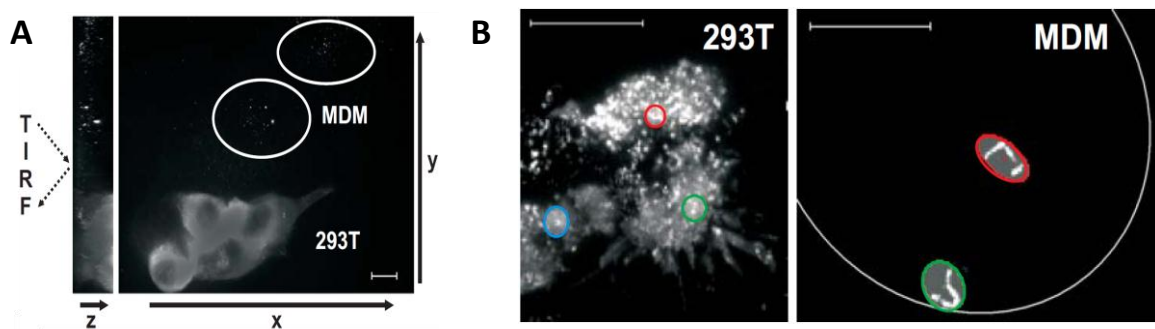


**Figure 6.10 TIRF analysis of HIV-1 GG infected macrophages and 293T cells.**

(A) HIV-1 GG infected macrophages (6 dpi) (marked by the white circle) and 293T cells (1 dpi) were cocultured and z-stacks of GFP/Gag expression recorded to confirm the presence of intracellular accumulations within the macrophages.

(B) The area shown in (A) was analyzed by TIRF over a period of four minutes. Depicted is a cropped 47 s interval in which Gag became apparent at the PM of a macrophage. The 747 individual images recorded during the 47 s observation were stacked to one image.

The scale bar shows a distance of 10  $\mu\text{m}$ .

When imaging the TIRF layer, thus only illuminating the first 200 nm of the plasma membrane, we detected a rich pattern of assembling Gag in 293T cells that were relative static over the imaging period of 4 minutes. These signals indicate Gag assembly and budding events at the plasma membrane like it was shown for HeLa cells (Ivanchenko et al., 2009). In strict contrast, fluorescence at the plasma membrane of HIV-1 GG infected macrophages was close to the background signal, which indicates the absence of HIV-1 assembly at the plasma membrane of macrophages (Figure 6.10 B). Nevertheless there were some very rare events of GFP signals that suddenly appeared, followed by fast movement and sudden disappearance. For quantitative analyses, 3 randomly defined regions of interest (ROI) were taken at the plasma membrane of 293T cells and the 2 regions of Gag appearance at the plasma membrane of macrophages. Then the relative GFP intensity was analyzed over time (Figure 6.11). While GFP intensity of the ROIs at the plasma membrane of 293T cells stayed stable over time, the appearance of GFP at the plasma membrane of macrophages happened within 700 ms. Based on the analysis of Ivanchenko et al., these events are too fast to resemble plasma membrane assembly. Thus, it is tempting to speculate that these particles have been previously assembled within the macrophage and were transported from the inner area to the plasma membrane of the macrophage.

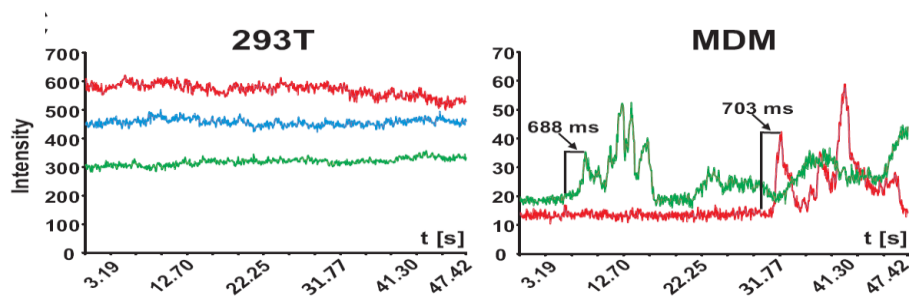


**Figure 6.11 TIRF analysis of HIV-1 GG infected macrophages and 293T cells.**

Randomly defined regions of interest (ROI) on the PM of 293T cells and the two areas of Gag appearance at the PM of macrophages were marked (colored eclipses in (B)) and relative fluorescence intensity displayed over time. Similar kinetic was observed of Gag appearance at the PM of HIV-1 GG infected macrophages from two other donors.

#### **4.5 HIV-1 within VCC are inaccessible to antibodies**

Several groups have demonstrated that HIV-1 is found in intracellular VCC in macrophages and it has been suggested that these compartments might shield HIV-1 from the humoral immune response (e.g. Benaroch et al., 2010; Deneka et al., 2007; Welsch et al., 2011). However, experimental proof supporting this hypothesis is still lacking. Furthermore, there is accumulating evidence suggesting that some of these VCCs can be connected to the plasma membrane by so called microchannels (Bennett et al., 2009; Welsch et al., 2011), which might allow passage of virions and antibodies.

To address antibody accessibility of VCCs the tetraspanin CD81 was analyzed as a known marker present within virus accumulations and within the envelope of mature HIV-1 particles (Grigorov et al., 2009). In addition it was postulated that CD81 as well as other tetraspanins serve as a gateway for HIV-1 (Nydegger et al., 2006) and there might be a direct interaction of Gag with CD81 as shown by immunoprecipitation in chronically HIV-1-infected T cells (Grigorov et al., 2009). To verify the interaction of Gag with CD81 in living cells a recently established FACS-based FRET assays was used (Banning et al., 2010). 293T cells that were transfected with Gag-CFP or HIV-1 Gag-CFP (HIV-1 GC) displayed a strong FRET signal with CD81-YFP (Figure 6.12).

Different controls were used to exclude false positive signals: First the unrelated membrane proteins CD4-YFP or Transferrinreceptor-YFP (TfR-YFP) were cotransfected with Gag-CFP or HIV-1 GC, but as expected these combinations did not result in FRET. Next a membrane-localized control construct MEM-CFP was used with CD81-YFP, CD4-YFP and TfR-YFP which did also not give a significant FRET signal, as it was the case with the remaining controls CFP only in combination with CD81-YFP, CD4-YFP and TfR-YFP (Figure 6.12).

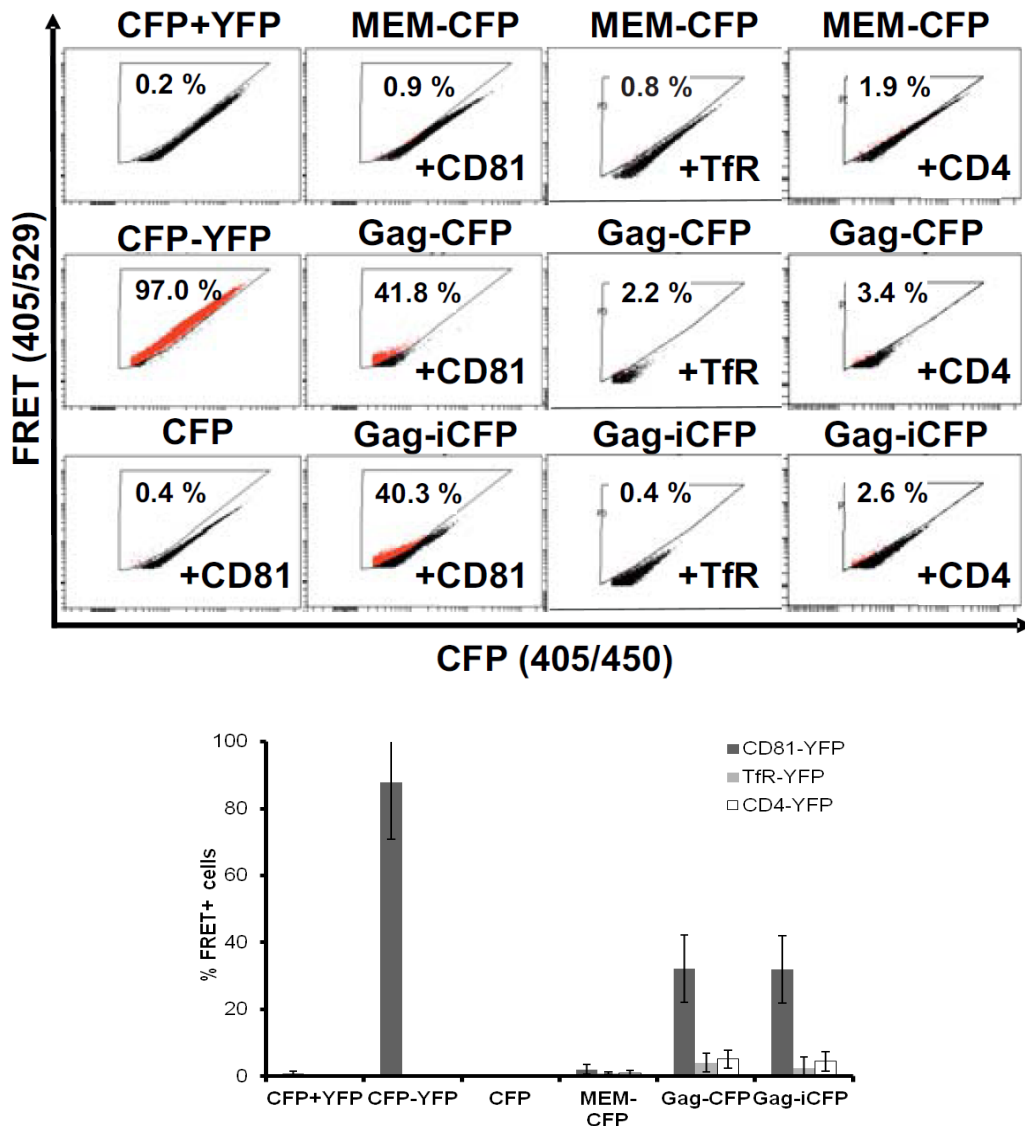


**Figure 6.12 FACS-FRET analysis of HIV-1 Gag with CD81, TfR, and CD4 in transfected 293T cells.**

Primary FACS plots show the percentages of cells scoring FRET positive. The graph displays mean values and SD from 4 to 10 independent transfections.

Post successful verification of CD81 associating with Gag an antibody was used against the extracellular (VCC internal) domain of CD81 to stain the VCC in HIV-1 GG infected macrophages. As expected, after fixation and permeabilization of infected macrophages (6 dpi) Gag strongly colocalized with CD81 ( $R=0.54$ ) (Figure 6.13). To analyze the surface accessibility of VCCs, living macrophages that were neither fixed nor permeabilized were incubated with anti-CD81 antibodies for 1 h at 4°C to prevent phagocytosis and inhibit membrane motility. Interestingly, only CD81 present at the surface of the macrophage could be stained, while VCCs could not be targeted by the antibody ( $R=-0.12$ ) (Figure 6.13).

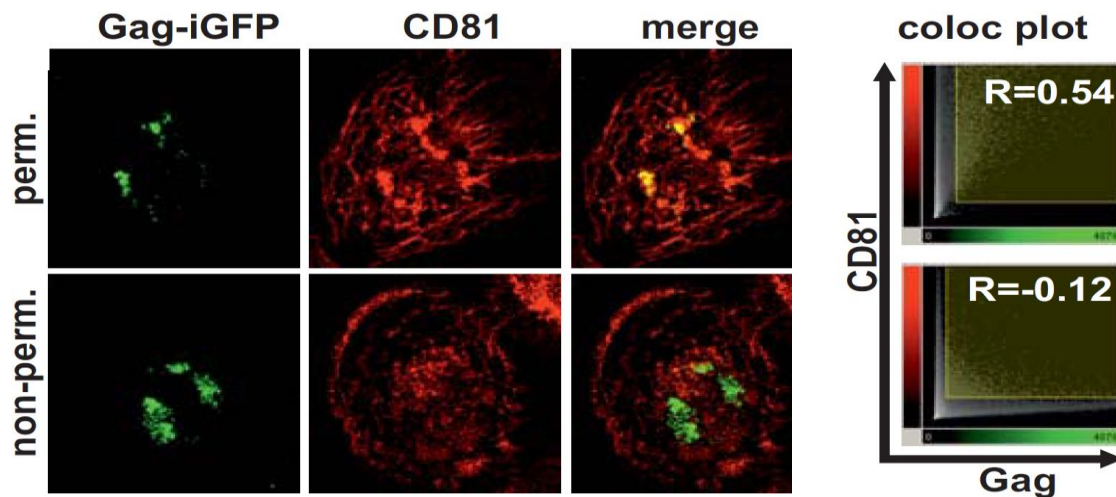


**Figure 6.13** The Gag assembly compartment in HIV-1 infected MDM is not accessible to antibodies at 4°C.

Permeabilized or untreated HIV-1 GG infected macrophages (6 dpi) were stained with anti-CD81 antibody at 4°C to label the HIV-1 assembly compartment and test accessibility toward antibodies. Confocal z-stacks of the macrophages were recorded to display maximum intensity projections and colocalization plots (Imaris 6.4.2; Bitplane). Pearson's correlation coefficient of Gag and CD81 antibody colocalization was also calculated with Imaris 6.4.2. Displayed are results from one out of four independent experiments.

To mimic the *in vivo* situation antibody feeding experiments were established at 37°C (Figure 6.14). Additionally, 3 different antibodies (2G12, VRC01, VRC03) were used against HIV-1 Gp120. These antibodies target the CD4 binding region of Gp120 and were reported to be broadly neutralizing (Trkola et al., 1996; Wu et al., 2010). For antibody specificity control also an antibody against the extracellular domain of TfR that does not inhibit the function of the receptor was used. When HIV-1 GG infected macrophages (6 dpi) were fixed and permeabilized before staining, Gp120 antibodies as well as CD81 antibodies reached the VCC and colocalized with Gag, confirming the functionality of these antibodies. In contrast, when living infected macrophages were incubated with antibodies for 1 h at 37°C only surface CD81 could be detected, which is in agreement with the previous results at 4°C. Furthermore, the broadly neutralizing Gp120 antibodies could not target macrophage internal virus accumulations (Figure 6.14 A). As a control transferrin receptor which is not part of the VCC and also not incorporated into virions was employed. Transferrin receptor antibody does not colocalize with Gag, neither in permeabilized nor untreated macrophages (Figure 6.14 B).

To quantify and statistically analyze the protection of macrophage internal HIV-1 towards antibodies, 25 infected and stained macrophages were imaged with the same intensity and the squared Pearson's correlation coefficient (R<sup>2</sup> value) was calculated with Bitplane Imaris 6.4. Except for the anti-TfR antibody, which did not colocalize with Gag, protection of VCCs from antibody accessibility was highly significant (Figure 6.14 C). Thus, macrophage internal HIV-1 is protected from recognition by broadly neutralizing antibodies.

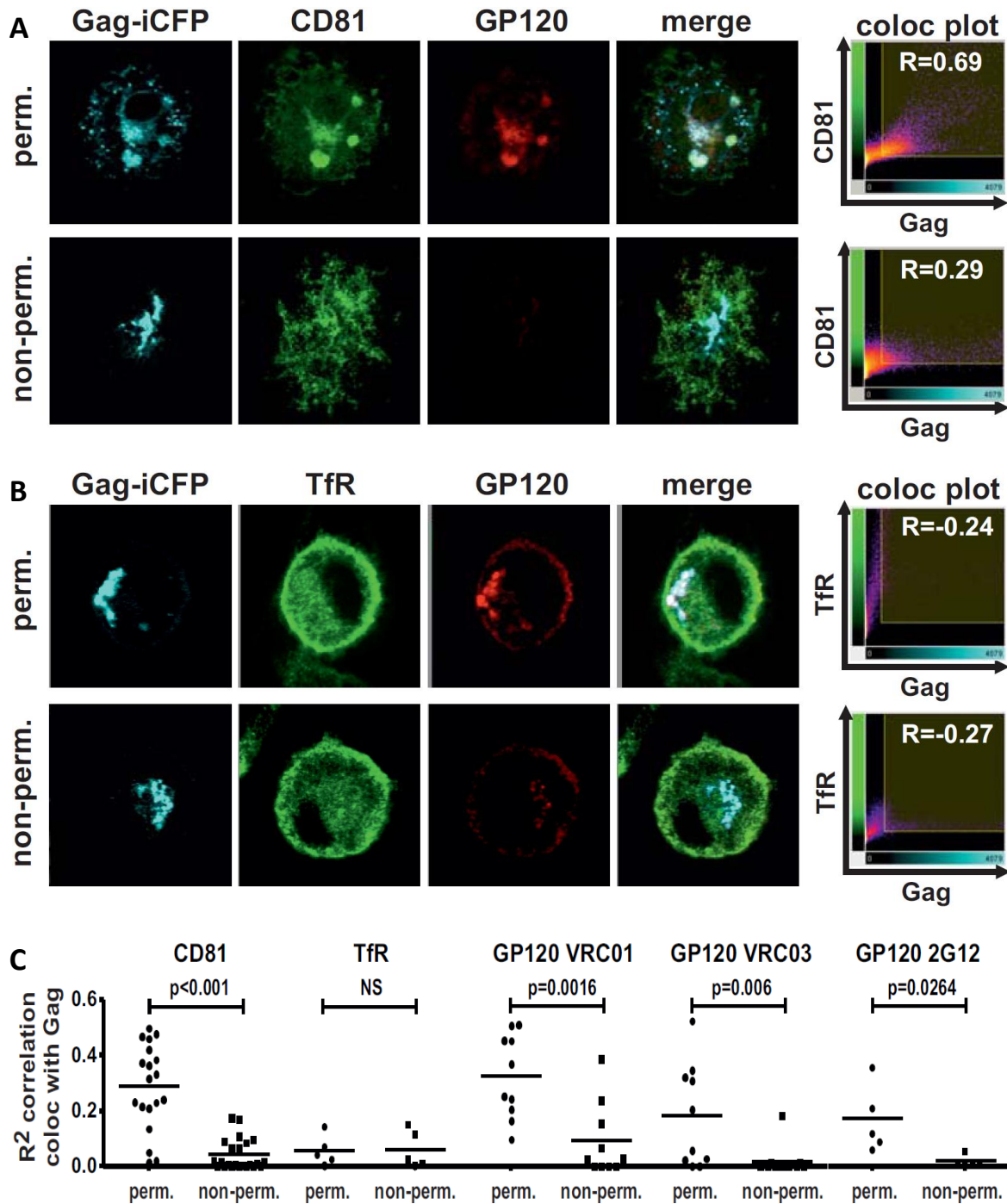


**Figure 6.14 HIV-1 within VCCs is protected from neutralizing antibodies.**

(A and B) HIV-1 GG-infected macrophages were either fixed and permeabilized or left untreated and incubated at 37°C with anti-CD81 (A) or anti-TfR (B) antibody and broadly neutralizing antibodies targeting GP120 as described in Materials and Methods. Fluorescently labeled secondary antibodies were used to detect sites of antibody binding. The Pearson's correlation coefficient of CD81, TfR, or GP120 antibody colocalizing with HIV-1 Gag was calculated with Imaris 6.4.2 (Bitplane).

(C) Confocal pictures of 25 macrophages were taken at the same intensities in order to be able to quantify and compare fluorescence. The squared Pearson's correlation coefficient values of CD81, TfR, or GP120 antibody colocalizing with HIV-1 Gag were plotted in the presented graph. A Student t test was done to assess statistical significance (Graph Pad Prism 5).



#### 4.6 HIV-1 is efficiently transferred from macrophages to T-cells

It has been demonstrated that HIV-1 produced by macrophages can be efficiently transferred to T cells via a so called virological synapses (Groot et al., 2008; Waki and Freed, 2010). This cell-to-cell transfer of HIV-1 is much more efficient than the infection with cell-free virus (Groot et al., 2008).

Using live cell microscopy it was possible to visualize cell-to-cell transfer from an infected macrophage to a T-cell (Figure 6.15). Primary macrophages were infected with HIV-1 GG. Three days post infection autologous PBLs were coincubated with the infected macrophages. 30 seconds after starting the imaging process, a T-cell (marked with an arrow) had already docked to an infected macrophage (surrounded by the blue circle in the first image) displaying a large intracellular Gag accumulation. Over an eight minute period HIV-1 GG was transferred to the T-cell, which harbored increasingly amount of GFP and hence Gag (Figure 6.15).

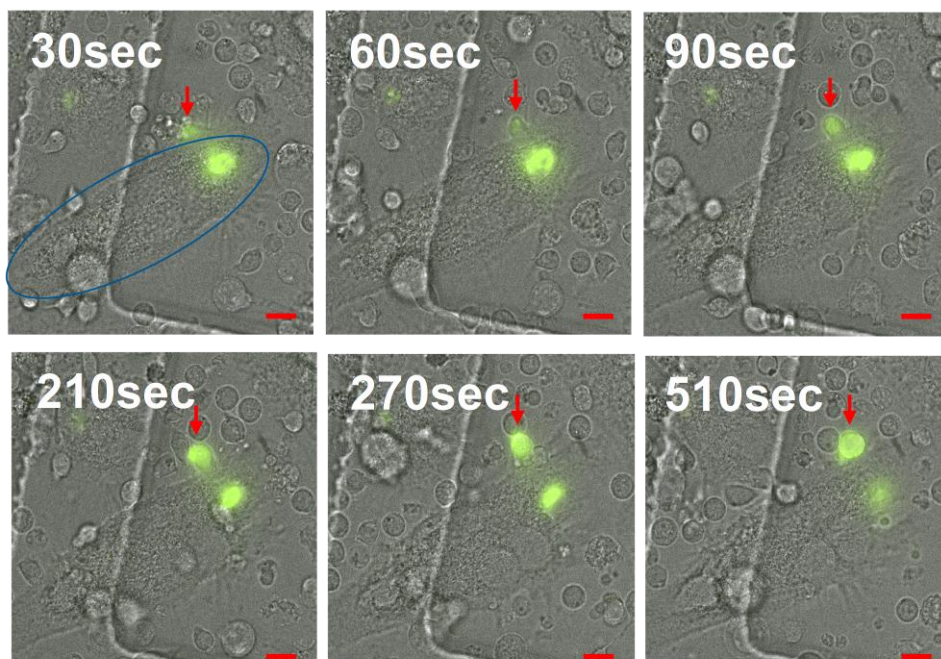


**Figure 6.15 Live Cell Imaging of HIV-1 GG transfer from MDM to PBMC.**

Three days post infection autologous PBMC were coincubated with HIV-1 GG infected MDM (surrounded by the blue circle) and observed by time-lapse fluorescence microscopy for a period of 8.5 min. To prevent photo bleaching images were recorded every 30 sec with a 60x Plan Fluor objective (Nikon). Red arrowheads indicate the docked PBL that is infected by cell-to-cell transfer.

The scale bar shows a distance of 10  $\mu$ m.

To verify the finding that HIV-1 stored in VCCs of infected macrophages is not accessible to antibodies and to investigate if cell-to-cell transfer from infected macrophages to adjacent cells is sensitive towards antibody neutralization, a functional experiment was set up (Figure 6.16). CemM7 T-cells were infected with R5-tropic HIV-1 in the presence of 20  $\mu\text{g}/\text{ml}$  HIV-1 Gp120 2G12 antibody, anti-TfR antibody or without any antibodies. As expected, the addition of 2G12 antibodies suppressed the infection nearly to background levels, whereas the addition of anti-TfR antibodies did not lead to a decrease of infection (Figure 6.16 A).

Next HIV-1 infected macrophages (6 dpi) were intensively washed and treated for 1 h at 37°C with 20  $\mu\text{g}/\text{ml}$  HIV-1 Gp120 2G12 antibody, anti-TfR antibody or without any antibodies. Then the antibodies were removed and macrophages were cocultured with CemM7 T-cells for 10 h at 37°C. Next CemM7 T-cells were harvested by 5 mM EDTA-PBS and cultured in new medium for 3 to 4 days. At these timepoints GFP expressing infected cells could be analyzed by FACS measurement (Figure 6.16 B). This experiment revealed that HIV-1 transfer from macrophages to T-cells is not inhibited by broadly neutralizing Gp120 antibody. Thus, HIV-1 is protected from the humoral immune system, but can be efficiently transmitted to T cells via cell-to-cell transfer.

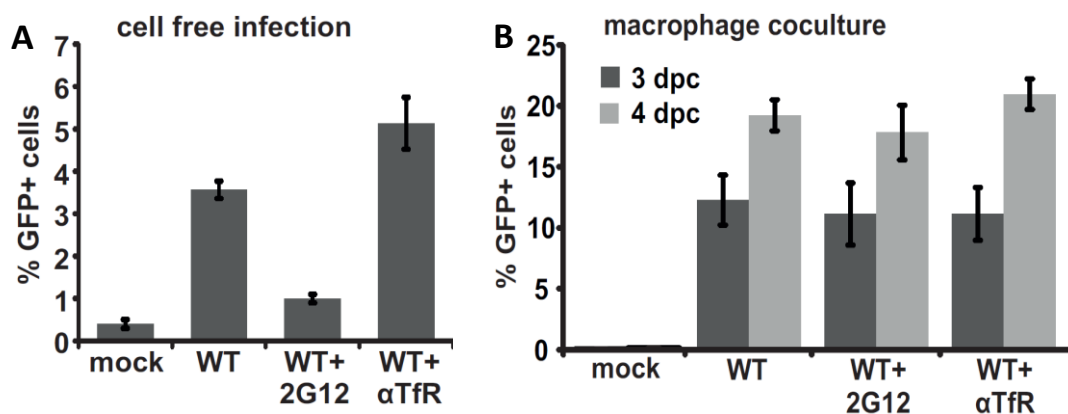


**Figure 6.16 Antibody preincubation does not suppress HIV-1 transfer from MDM to T-cells.**

(A) A total of 100 000 CemM7 T-cells were incubated with 20 ng of p24 from R5-tropic HIV-1 GFP and 20  $\mu\text{g}/\text{ml}$  of the indicated antibodies for 12 h in a total volume of 200  $\mu\text{l}$ . Then, 500  $\mu\text{l}$  RPMI was added and cells were cultured for two additional days. The number of GFP-positive cells was assessed by FACS measurement. Displayed are mean values and SD from results of three independent infections.

(B) A total of 50 000 macrophages were infected with R5-tropic HIV-1 GFP and pretreated for 1 h with 20  $\mu\text{g}/\text{ml}$  of the indicated antibodies at 37°C. Then, antibodies were removed and macrophages were cocultured for 10 h with CemM7 cells. CemM7 were subsequently collected by 5mM EDTA-PBS and cultured for another 3 or 4 days. The number of GFP-positive cells was assessed by FACS. The graph shows means and standard errors of the means (SEM) from results of infections of macrophages from three different donors with two independent virus stocks.

#### 4.7 The spatial organization of an internal Gag accumulation

Electron microscopical analyses showed that VCCs can be connected to the plasma membrane via so called microchannels (Bennett et al., 2009; Welsch et al., 2011). These experiments also indicated that not all VCCs are membrane connected and the spatial expansion of such structures is still not entirely resolved. Primary macrophages exert multiple restrictions towards HIV-1 resulting in varying infection rates between donors ranging from 2 to 10% using R5-tropic HIV-1 NL4-3 (Schindler et al., 2010; Schindler et al., 2007; Laguette et al., 2011). Correlative fluorescence/electron microscopy was used to identify infected macrophages and to specifically image VCCs (Figure 6.17). Macrophages were infected with HIV-1 GG in a dish with imprinted relocalization grid and 7 dpi infected cells were imaged by fluorescence microscopy. Using the relocalization grid of the dish allowed to reidentify macrophages by electron microscopy which were imaged before by fluorescence techniques. The macrophage depicted in Figure 6.17 A harbored 2 Gag accumulations marked by the red and the white asterisk. Closer investigation of the first accumulation (red asterisk) revealed a membranous web like structure surrounded by six vacuoles which seemed to be in contact with the web. HIV-1 particles (indicated by red arrows) could be found in the vacuoles as well as in the web like structure although less frequent (Figure 6.17 B). Such web like structures were never found in uninfected macrophages.

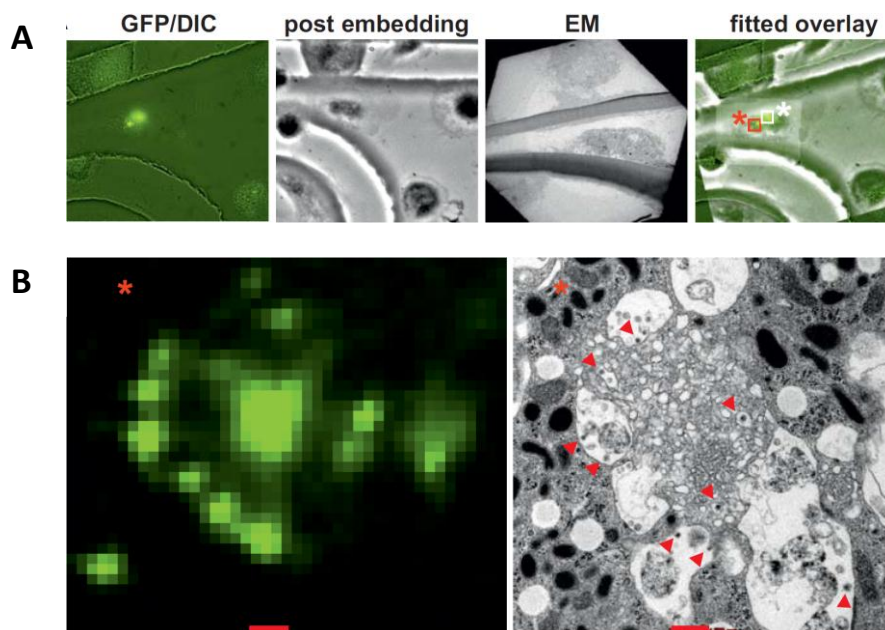


**Figure 6.17 Correlative microscopy of macrophage internal HIV-1 accumulations.**

(A) Relocation of an HIV-1 GG-infected macrophage by correlative microscopy. Fluorescence images of infected macrophages grown on a culture dish with a grid were taken to relocate the infected macrophage by EM 7 dpi. The scale bar shows a distance of 10  $\mu\text{m}$ .

(B) Magnification of the area of Gag accumulations, marked with a red square and an asterisk in panel (A), and the ultrastructure of this specific region by EM. Some viral particles are marked with a red arrowhead. The scale bar indicates a distance of 500 nm.

To analyze the spatial expansion of the web like structure and the surrounding vacuoles, serial sections of the whole second Gag accumulation (white asterisk) were carried out and the images of the sections were 3D reconstructed using Bitplane Imaris 6.4 (Figure 6.18). To discriminate different vacuoles and the central web, they were marked with different colors and the viral particles were visualized as yellow dots. This VCC was build up of 7 different vacuoles and a web like structure (light green; turquoise) in the center of the complex. The web like structure and all the vacuoles were membrane enclosed and separated from each other, although a possible connection by microchannels cannot be excluded; only one virus containing vacuole, colored in blue, reached the microvilli-plasma membrane area at the top of the macrophage (Figure 6 18).

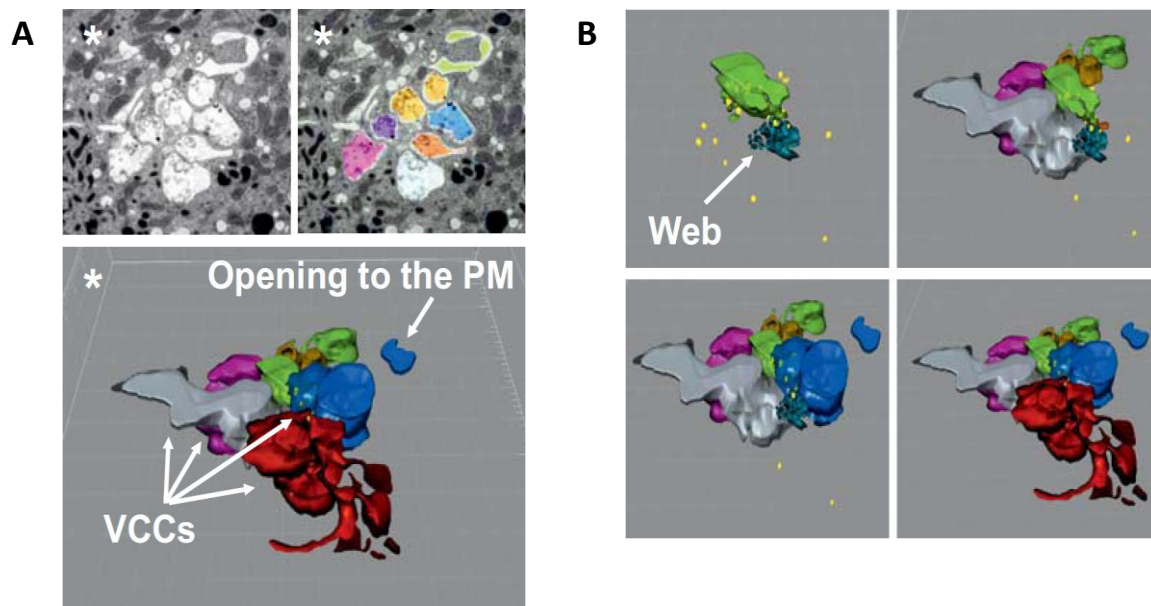


**Figure 6.18 Three-dimensional reconstruction of the serial EM sections of a VCC.**

(A) 3-D reconstruction of the serial sections of VCC displayed in Figure 6.17 A (white asterisk). Bitplane Imaris 6.4.2 was used to reconstruct the colored vacuoles surrounding the central membranous web region. Viral particles are depicted as yellow dots. One large VCC, colored in blue, ends up toward a microvillus-enriched region.

(B) The membrane web in light green and turquoise (first picture) is surrounded by VCCs. Viral particles (yellow dots) are present inside. Similar structures corresponding to Gag accumulations were observed in two additional macrophages from this donor and in two macrophages from independent donors. We never found comparable structures in uninfected macrophages from the same donors.

#### 4.8 Gag alone is able to form VCC-like expression pattern

Formation of VCCs could be dependent on viral proteins other than Gag. However in T-cells and different cell lines HIV-1 Gag by itself is able to form virus like particles (VLP) that are similar to immature viruses but contain empty capsid or randomly incorporate cellular proteins and RNA (Gousset et al., 2008; Waki and Freed, 2010).

To investigate if Gag-alone is sufficient to form VCCs, primary macrophages were electroporated with Gag-CFP by Amaxa nucleofection. One day post electroporation cells were fixed and analyzed by confocal microscopy. Figure 6.19 shows macrophages of 2 different donors that express Gag-CFP in large intracellular Gag accumulation similar to macrophages infected with full length HIV-1. Thus, Gag by itself is able to accumulate intracellular and form VCC in macrophages without the participation of other viral proteins.

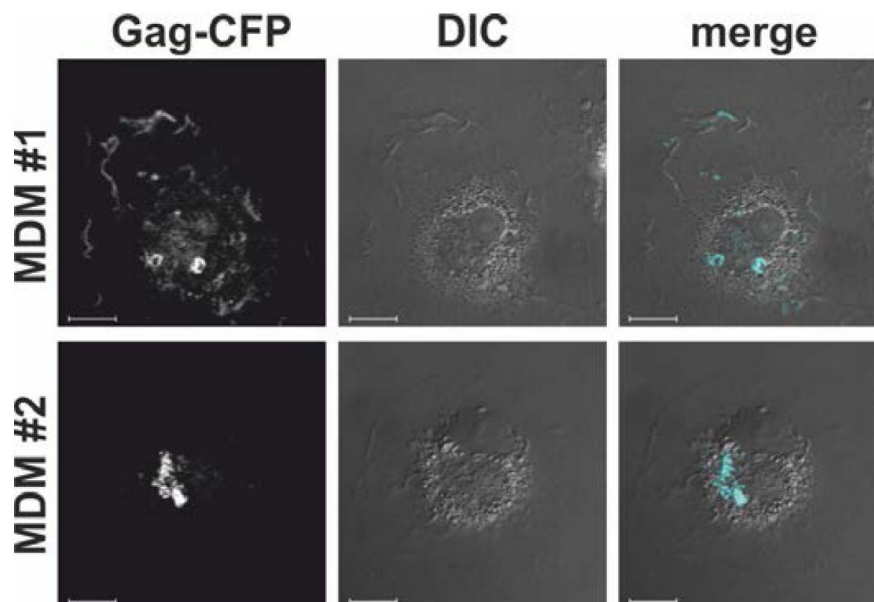


**Figure 6.19 Expression of Gag-CFP in macrophages.**

A Gag-CFP expression plasmid was electroporated into macrophages by nucleofection following the macrophage protocol provided by the manufacturer (Amaxa). One day post nucleofection macrophages were analyzed for CFP expression by confocal microscopy. Shown are two representative examples of nine recorded cells. The scale bar indicates 10  $\mu$ m.

#### 4.9 Gag interacts with tetraspanins found in VCCs

Gag alone is sufficient to induce VCCs and it has been previously demonstrated that Gag associates with the tetraspanin CD81. In T-cells HIV-1 buds at the plasma membrane from tetraspanin enriched microdomains (TEM) and viral envelopes contain CD81, CD82 and CD63 (Grigorov et al., 2009). Furthermore it was demonstrated that CD9 and CD53 seem to be present in VCCs (Deneka et al., 2007). Since tetraspanins interact with each other, form homo and heteromers and are membrane associated, one hypothesis is that Gag could induce formation of the web by interaction with multiple tetraspanins.

Therefore, FACS-based FRET was used to find possible interactions between tetraspanins besides CD81 and Gag (Figure 6.20). Gag-CFP was cotransfected with the YFP tagged tetraspanins CD9, CD53, CD82 and as an internal positive control CD81. To prevent false positive signals the MEM-CFP construct and CFP only are cotransfected as controls. Interestingly, Gag specifically interacted with CD82 and CD9 in addition to CD81, but not with CD53, although all four proteins were found in VCC (Deneka et al., 2007; Grigorov et al., 2009) (Figure 6.20).

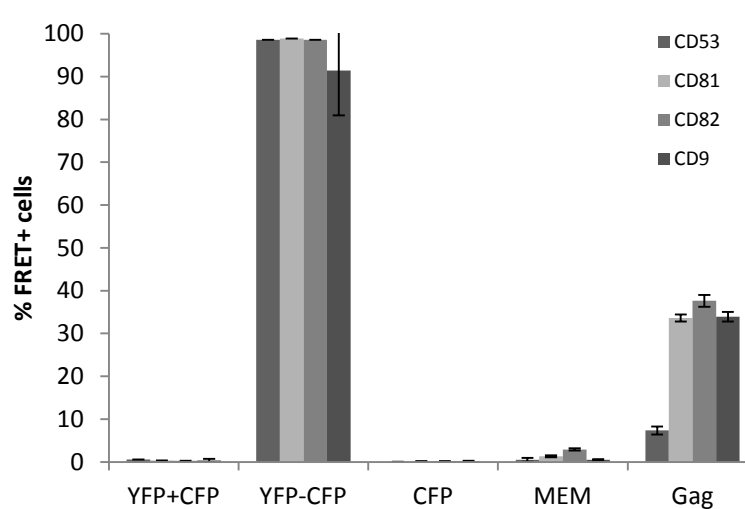


**Figure 6.20 FACS-FRET analysis of HIV-1 Gag with the tetraspanins CD81, CD82, CD53 and CD9 which are located in VCC.**

The graph displays mean values and SD from 3 to 10 independent transfections.

This data suggests that TEMs might form in macrophage internal VCCs and serve as a budding platform similar to T-cells (Nydegger et al., 2006).

## 5 Discussion

More than 30 years since the first cases of AIDS were reported in the USA, HIV-1 became the new plague and killed more than 25 million people throughout the world. Today it is possible to suppress viral loads under the detection level, however patients have to be treated lifelong and it is still not possible to cure the infection. The reason for this is HIV-1 persistence in cellular reservoirs, mainly CD4+ memory T-cells in the bone marrow and macrophages. HIV-1 infected macrophages might also carry the virus into the central nervous system by passing the blood-brain barrier and therefore causing HIV-1 associated neuronal diseases.

The mechanism of HIV-1 persistence in macrophages is not clear. Furthermore the late phase of HIV-1 replication in macrophages is unclear, especially the exact process of virus assembly and budding. The aim of this thesis was to analyze the late phase of HIV-1 in primary human monocyte-derived-macrophages. By the use of a newly generated GFP tagged HIV-1 construct replicating in primary macrophages, the formation of virus containing compartments (VCC) and their accessibility via cell surface-administered antibodies was investigated. GFP tagged HIV-1 is a powerful tool to analyze Gag assembly in macrophages

Fluorescently labeled viruses have been proven to be important tools to analyze the HIV-1 replication cycle (Hübner et al., 2009; Jouvenet et al., 2006; Muller et al., 2004). Such virus constructs allow to analyze the trafficking of viral protein or even assembled virions in living cells.

Within this thesis a GFP tagged HIV-1 construct was generated that is able to infect and replicate in macrophages, although HIV-1 GG is attenuated in comparison to wild type. In contrast to other virus constructs that also harbor GFP between p17 matrix and p24 capsid of the Gag polyprotein, in HIV-1 GG the GFP cassette is flanked by two HIV-1 protease cleavage sites (Jouvenet et al., 2006; Muller et al., 2004). While the GFP-tag normally results in uninfected particles, the insertion of the protease cleavage sites leads to infectious virions, because GFP is released during HIV-1 maturation (Hübner et al., 2007). The prototype of HIV-1 GG designed by the group of Chen has been elegantly used to analyze transfer and trafficking of HIV-1 across virological synapses of electroporated T-cells (Hübner et al., 2009). Although this construct is a nice tool, its use is hampered by the fact that it spreads poorly in most cell lines and primary cells (Hübner et al., 2007). In contrast to this virus the newly constructed HIV-1 GG is R5 tropic, infects CCR5 positive cells and spreads and replicates in macrophages. Although infection efficiency is 2-3 fold reduced in comparison to the wild type, HIV-1 GG shows the same Gag localization in macrophages in comparison to the wild type and also the replication kinetic is similar to the untagged version (Figure 6.2 & 6.4 A, B).

The advantage of this construct is strengthened by the fact that since now the only tagged R5 tropic virus that is able to infect and replicate in macrophages is an HIV-1 AD8 variant with a tetracycline (TC) tag (Gousset et al., 2008). This construct introduced by Freed's lab is a powerful tool because the TC tag has only a minor impact on virus infectivity and it was successfully used to show that macrophage internal HIV-1 was rapidly transported to the VS between an infected macrophage and a T-cell. The disadvantage of this construct is its need for biarsenic labeling, which is tedious and hampers the possibility to image the formation of newly synthesized Gag.

### **5.1 HIV-1 Gag assembles in intracellular virus containing compartments**

In contrast to CD4<sup>+</sup> T-cells where HIV-1 buds at the plasma membrane the localization of HIV-1 assembly sites in macrophages is controversially discussed (Benaroch et al., 2010; Welsch et al., 2007). In macrophages HIV-1 is found in membrane enclosed structures designated virus containing compartments (VCC) (e.g. Gendelman et al., 1988; Raposo et al., 2002). Despite intense investigations the exact nature of these compartments is elusive, since marker proteins present in VCCs do not give an exact clue on the origin of these structures. In addition, the intracellular location of VCCs has been questioned, because it was demonstrated that VCCs are accessible to membrane impermeant tracers like ruthenium red (RR) and HRP (Deneka et al., 2007; Welsch et al., 2007). One of the reasons why it has been difficult to define the place of HIV-1 assembly in macrophages is due to the lack of a dynamic view on Gag synthesis (Benaroch et al., 2010).

Formation of HIV-1 assembly sites in macrophages was investigated in this thesis by i) imaging of the infection process of macrophages with HIV-1 GG up to 4 days post infection (Figure 6.7), ii) 2D- and 3D-imaging of HIV-1 GG infected macrophages (Figure 6.6 & 6.8) and iii) TIRF microscopy of the plasma membrane of HIV-1 GG infected macrophages (Figure 6.10). In sum, these experiments demonstrate formation of internal Gag accumulations without appearance of Gag at the plasma membrane of HIV-1 infected macrophages. These results and the identification of budding events at the limited membrane of VCCs support the hypothesis that HIV-1 can assemble in a macrophage internal compartment. In addition, the plasma membrane seems not to be the major assembly site, although it cannot be fully excluded that some HIV-1 assembly occurs at the plasma membrane. Furthermore one scenario could be that Gag assembly is initiated at the plasma membrane and finalized in internal compartments. In this context it is noteworthy that faint Gag and smaller Gag puncta were found at the plasma membrane. The main evidence for absence of HIV-1 assembly at the plasma membrane of macrophages was derived from TIRF experiments. However this technique only visualizes the bottom of polarized cell, which might result in failure to detect deeper membrane invaginations. On the other hand TIRF was elegantly used to analyze the temporal



procedure of HIV-1 budding at the plasma membrane of HeLa cells and 293T cells (Figure 6.10 and Ivanchenko et al., 2009).

Importantly, the results of this thesis do not exclude the possibility that some VCCs in macrophages might be connected to the plasma membrane for example by microchannels (Bennett et al., 2009; Welsch et al., 2011). In a recent study by the lab of Sattentau using electron tomography and EM with stereology, a complex membranous network was found harboring viral particles. Some of these VCCs were connected to the cell surface by tubelike structures with insufficient diameter for virion passage (Welsch et al., 2011). This is in contrast to Bennett et al showing long microchannels with some channels of sufficient diameter for virion passage (Bennett et al., 2009). Such structures cannot be visualized by TIRF microscopy and serial sectioning with subsequent 3D reconstruction fails to display such narrow structures. Thus, some VCCs might be located deep inside the macrophage, but connected to the plasma membrane by small microchannels.

In sum, the data of this thesis suggests that the majority of the plasma membrane of HIV-1 infected macrophages is free from budding sites. This is strengthened by the absence of identified assembly and budding sites at the plasma membrane in a number of published EM studies, whereas such profiles were frequently detected in VCCs (Figure 6.17 & 6.18 and Jouve et al., 2007; Pelchen-Matthews et al., 2003). As mentioned before, Gag assembly might be initiated at plasma membrane invaginations of infected macrophages, but this leads to the question how this process is mechanistically organized to confer specificity. In contrast to this, the studies of Bennett et al. and Welsch et al. demonstrate that VCCs are partly deep inside the macrophage, but can be connected to the plasma membrane by small tubules or microchannels (Bennett et al., 2009; Welsch et al., 2011). These finding could explain the partial accessibility of VCCs with small membrane impermeant tracers like ruthenium red and the neutral pH inside virus-containing vacuoles (Welsch et al., 2007; Jouve et al., 2007).

## **5.2 Virus containing compartments are protected from antibodies**

It is postulated for long that macrophage internal budding of HIV-1 might resemble an immune evasion mechanism (Deneka et al., 2007; Welsch et al., 2011). However, direct experimental proof is lacking and the finding of microchannels connecting VCCs to the cell surface as well as potential plasma membrane assembly of HIV-1 in macrophages further raised doubt in this theory (Deneka et al., 2007; Bennett et al., 2009; Welsch et al., 2011). Microchannel diameter is discussed controversially. One study postulated a diameter big enough for virion and antibody passage (Bennett et al., 2009), whereas Welsch and colleagues reported a tubule diameter of less than 100nm. In addition, they showed that these structures are grouped in a convoluted manner which would limit antibody diffusion (Welsch et al., 2011). Deneka and colleagues found similar channels

with a diameter of 20nm. They postulate that RR ( $M_r = 786$ ) and HRP (40 kD) are small enough to pass through these connections, whereas trafficking of antibodies (10nm) or viral particles (120nm) might be inhibited.

This thesis provided for the first time experimental proof demonstrating that macrophage internal HIV-1 cannot be targeted by antibodies (Figure 6.13 & 6.14). Experiments were performed in living primary human monocyte-derived macrophages, presenting the best *in vitro* model for macrophage research. Furthermore macrophages were infected with replicating HIV-1 expressing all viral proteins in the natural context. Antibody accessibility experiments were based on the usage of four different antibodies, either against HIV-1 Gp120, or against the tetraspanin CD81, that is known to be present in VCCs and might play an important role in HIV-1 assembly (Figure 6.13 & 6.14 and Deneka et al., 2007; Nydegger et al., 2006). All HIV-1 Gp120 antibodies are directed against the CD4 binding site of Gp120 and are described as broadly neutralizing against a large spectrum of HIV-1 strains with no cross-reactivity against host self or other antigens (Trkola et al., 1996; Wu et al., 2010). First experiments were done at 4°C to prevent phagocytosis and membrane motility stabilizing existing openings toward the plasma membrane. To additionally mimic the *in vivo* situation the experiments were repeated at 37°C allowing endocytic uptake and presumably transient openings of VCC toward the plasma membrane. Importantly, at 4°C and also at 37°C antibodies are unable to target VCCs or HIV-1 Gag in non-permeabilized cells. Thus, HIV-1 in VCCs is protected from antibodies, also explaining previous results demonstrating that macrophages can harbor infectious virions over several weeks (Sharova et al., 2005).

Importantly macrophages are one of the main productive viral reservoirs and are able to evade elimination by the immune system. In addition, HIV-1 infected macrophages take the virus across the blood-brain barrier and cause HAND (Maung et al., 2011; Alexaki et al., 2008). The findings within this thesis emphasize the advantage of macrophage internal HIV-1 production at low levels, without antibody neutralization. Infected macrophages serve as hidden virus factories transmitting the virus into the CNS and other organs.

### **5.3 Neutralizing antibodies cannot prevent HIV-1 cell-to-cell transfer**

Cell-to-cell spread of HIV-1 is far more efficient than infection by cell-free virions (Carr et al., 1999; Phillips et al., 1998) and takes place at macromolecular adhesive contact sites named virological synapses (VS). Furthermore it is suggested that this form of virus transmission is the main route *in vivo*, where most of the viral spread takes place in lymph nodes and other lymphatic organs (Martin et al., 2010). Although cell-to-cell spread between CD4+ T-cells was intensively investigated in the last years, little was known about macrophages (e.g. Hübner et al., 2009). During the last 5 years two groups could independently show that infected macrophages are able to transfer HIV-1 to uninfected

CD4+ T-cells across virological synapses (Groot et al., 2008; Waki and Freed, 2010). Freed's lab showed by the use of a TC tagged HIV-1 construct that after docking of a CD4+ T-cell to an infected macrophage, internal stored virions were rapidly transported to the VS (Waki and Freed, 2010). The group of Sattentau analyzed the VS between infected macrophages and CD4+ T-cells by pretreatment of target cells with different blocking antibodies or fusion inhibitors. They could show that blocking the Gp120 interaction surface at the CD4 receptor prevents efficient transfer of HIV-1 to CD4+ T-cells (Groot et al., 2008). This finding is important because the need of Env for cell-to-cell transfer proves that viral particles are released before infection of the target cell. During this short "cell free" status the transmitted virus could be vulnerable to neutralizing antibodies. Importantly, it has been demonstrated that cell-to-cell transfer of HIV-1 transmitted between CD4+ T-cells can be suppressed by neutralizing antibodies (Martin et al., 2010). The findings from CD4+ T-cells cannot predict the possible inhibition of HIV-1 transfer by VS between macrophages and CD4+ T-cells. As discussed, in T-cells HIV-1 assembles at the plasma membrane and Env located at the plasma membrane is prone towards neutralization during the budding process.

Interestingly, the results from this thesis not only demonstrate that macrophage internal HIV-1 is protected from antibodies, but also establish that efficient cell transfer occurs despite antibody treatment (Figure 6.16 B). This demonstrates on a functional level antibody protection of HIV-1 in macrophages and due to the absence of Env from the plasma membrane further suggests macrophage internal assembly of HIV-1. Interestingly, electron tomography studies of VS between CD4+ T-cells suggested that these are relatively permeable structures (Martin et al., 2010). Thus, further experiments have to address the question if efficient cell-to-cell transfer from macrophages to T-cells is possible in the presence of neutralizing antibodies and if VS between macrophages and T-cells differ in structure.

#### **5.4 HIV-1 is sequestered into a macrophage internal membranous web**

Correlative microscopy experiments allowing to reconstruct the 3D structure of the VCC demonstrated that VCCs are not just one large vacuole filled with viral particles. In contrast, virus accumulations consist of different large vacuoles which were grouped around or in close contact to a membranous web (Figure 6.17). This membranous web was described before and called spongelike structure (Deneka et al., 2007; Benaroch et al., 2010). While Deneka and colleagues reported that such structures are rarely found by standard EM techniques, Benaroch published that they are frequently found in infected macrophages. Both studies suggest that these structures have to be connected to the plasma membrane because of the accessibility to RR. The accessibility of VCC to small molecules like RR ( $M_r = 786$ ) or HRP (40kDa) is explained by the finding of narrow tubules connecting at least some of the virus containing vacuolar structures to the plasma membrane and to

the central membranous web (Deneka et al., 2007; Bennett et al., 2009; Welsch et al., 2011). EM analysis conducted within this thesis could not identify such connections; however the close vicinity of the vacuolar structures and the membranous web suggests a possible connection. It is important to notice that viral particles can be found in the “vacuoles” as well as inside the membranous web, whereas budding profiles are only found in the membrane enclosed structures surrounding the sponge. Although it is problematic to interpret EM pictures in a moving context, it can be speculated that the “vacuoles” are the site of virus assembly and released virions are transported by the membranous web to the cell surface.

The group of Mark Marsh intensively investigated the composition of VCCs (Deneka et al., 2007). They initially observed that VCCs are positive for the tetraspanins CD81, CD9, CD53 and CD63 and subsequently analyzed uninfected macrophages to find a compartment harboring such markers. Although CD63 was only present in late endosomes and lysosomes, CD81/CD9/CD53 positive vesicles with diameters of 2-3  $\mu\text{m}$  were detected. When Env alone was expressed, these structures also lacked CD63, leading to the conclusion that CD63 might be recruited to this compartment by Gag or other viral proteins. EM studies of the same group additionally suggested the presence of small sponge like structures in uninfected macrophages, but in infected macrophages the CD81/CD9/CD53-containing structures are enlarged and irregular (Deneka et al., 2007). Importantly, a lot of groups reported budding events at the limiting membrane of VCC but not at the surface of macrophages. This is remarkable, since CD81 and other tetraspanins are also present at the cell surface (Figure 6.13 & 6.14; and e.g. Deneka et al., 2007; Benaroch et al., 2010; Welsch et al., 2011).

Interestingly, tetraspanins also play a role in HIV-1 storage in dendritic cells (DC). Although mature DCs cannot be productively infected by HIV-1, they can capture free virions, collect them in CD81/CD9 positive intracellular areas and release them via trans infection of T-cells (Kwon et al., 2002; McDonald et al., 2003). These HIV-1 storage compartments normally play a role in antigen presentation and it was shown that in DCs MHC class II receptors are associated with CD9, CD53, CD81 and CD63 (Engering and Pieters, 2001). Macrophages as professional APCs might also have such structures, but in contrast to DCs macrophages present only phagocytosed and processed antigens to T-cells. Because macrophages, in contrast to DCs, can be productively infected, HIV-1 might hijack the antigen processing storage compartment as cellular hideout. This hypothesis is supported by studies connecting CD81, CD53 and CD9 to the formation or activity of immunological synapses. Interestingly, formation of VS by HIV-1 competes with immunological synapse formation (Deneka et al., 2007; Kremontsov et al., 2009).

In sum, besides the unclear and still not fully resolved nature of the HIV-1 budding and assembly compartment the architecture of this structure, i.e. convoluted and large membrane invaginations, might aid in antibody evasion of internally sequestered HIV-1.

### **5.5 Gag interaction with tetraspanins might be sufficient to induce intracellular accumulations in macrophages**

CFP tagged Gag alone is also able to accumulate in internal regions comparable to Gag localization in HIV-1 infected macrophages (Figure 6.19). Although EM analysis of the Gag induced accumulation is lacking, it seems that Gag alone is able to form the membranous web like structure. This hypothesis is supported by the fact that Gag by itself is able to form virus like particles (Gousset et al., 2008; Waki and Freed, 2010). Furthermore, a recent report suggests that Gag alone induces the coalescence of lipid rafts and tetraspanin enriched microdomains in HeLa cells, which is important for HIV-1 budding (Hogue et al., 2011). Thus, different lines of evidence point towards Gag being the main player in induction of VCCs in macrophages.

The FACS-based FRET experiments demonstrated that HIV-1 Gag interacts with the cytoplasmic region of CD81, confirming studies reporting this interaction by coimmunoprecipitation in chronically HIV-1 infected T-cells (Grigorov et al., 2009). Since Gag itself might induce VCCs and these structures are positive not only for CD81, but also for CD9, CD53 and CD82 interaction of Gag with these tetraspanins was also assessed. Of note, Gag interacts with CD9 and CD82, but not with CD53 (Figure 6.20). CD9, CD63, CD81 and CD82 were suggested to build a gateway for HIV-1 in HeLa cells and T-cells (Nydegger et al., 2006; Grigorov et al., 2009; Jolly and Sattentau, 2007). However, the relative importance of CD63 is questionable, since lack of this tetraspanin had no effect on particle release, virion infectivity or the localization of the viral assembly site (Ruiz-Mateos et al., 2008). Therefore it was speculated that CD63 is only accidentally incorporated into HIV-1 particles by cycling between late endosomes and the cell surface via the CD81/CD9/CD53 compartment (Deneka et al., 2007). Despite these findings it seems unlikely that CD63 is incorporated accidentally into HIV-1 particles, raising the question for a yet undiscovered *in vivo* relevance of CD63 within progeny virions.

Gag interacts with CD9 although this tetraspanin is not incorporated into the virion (Grigorov et al., 2009). Thus, while CD9 might be important for HIV-1 assembly it could be dispensable for the budding procedure. Of note, K41, a CD9-specific antibody was able to inhibit the release of HIV-1, whereas release of influenza virus was not suppressed (Khurana et al., 2007). Treatment with K41 leads to a rapid relocation and clustering of CD9 at cellular contact sites. Importantly, also other tetraspanins CD81, CD82 and CD63 were present in these CD9-K41 clusters, suggesting that K41 modified the whole TEM leading to the loss of the HIV-1 assembly platform (Singethan et al., 2008). CD9 might have adopted a special role for HIV-1 production in macrophages, since primary CD4+ T-

cells only express low amounts of CD9 (Jolly and Sattentau, 2007). Treatment of HIV-1 infected T-cells with antibodies against CD81 and CD82 also had suppressive effects on HIV-1 release (Grigorov et al., 2009). In contrast, another study performed siRNA mediated knock down of CD9, CD63 or CD81 which did not result in suppression of HIV-1 release from HeLa cells (Krementsov et al., 2009). Furthermore, overexpression of these 3 tetraspanins impaired HIV-1 infectivity. Overexpression of CD63 lead to reduced cell-to-cell transfer to T-cells and knock down of CD81 reduced cell-to-cell transfer, although overexpression of CD81 had no effect (Krementsov et al., 2009).

These reports highlight the difficult and multifaceted role of tetraspanins in the biology of HIV-1. As a family of adaptor proteins they exert multiple interactions, have different functions in different cell types and can have complementary functions (Martin et al., 2005; Nydegger et al., 2006; Tarrant et al., 2003). Therefore, tetraspanins might be important not only for HIV-1 egress but also for entry. In the context of HIV-1 assembly in macrophages, the specific functions of the three tetraspanins CD81, CD82 and CD9 have to be investigated in further studies. Especially in the highly complex field of tetraspanins it is important to verify cell line data in primary cells, particularly in CD4+ T-cells and macrophages. The data of this thesis lead to speculations that tetraspanins are hijacked by HIV-1 Gag either because tetraspanins interact with parts of the budding machinery or to be transported to a distinct area at the plasma membrane where assembly is possible. Interestingly, colocalization of CD81 and CD9 in uninfected macrophages occurs only in vesicle-like structures and not at the plasma membrane (Deneka et al., 2007). This localization of CD81, CD82 and CD9 in concert with other tetraspanins and partner proteins can force HIV-1 to assembly at such intracellular structures. These structures might be absent from the plasma membrane and result in internal assembly. It is important to investigate which parts of the budding machinery interact with which tetraspanin or with Gag. Furthermore, due to its analogy to the virological synapse, tetraspanins might also be involved in the formation of the immunological synapse.

## 6 Conclusion

Interpretation of the results of this thesis in the context of recent investigations of other groups leads to speculations about the origin of internal HIV-1 accumulations in macrophages and the benefit for the virus. In uninfected macrophages small vesicle-like structures exist, which might be connected to the plasma membrane by narrow tubules (Bennett et al., 2009; Welsch et al., 2011). Characterization studies of VCCs indicate that they are not part of the endosomal pathway, but the presence of MHC-II and some tetraspanins implies a possible link to the antigen presentation ability of macrophages (Deneka et al., 2007; Raposo et al., 2002, Pelchen-Matthews et al., 2003). HIV-1 might hijack the MHC-II antigen presentation pathway and exploit it for budding and release. One reason could be that at the surface of macrophages some essential parts of the budding machinery might be missing or macrophage specific antiviral factors could suppress HIV-1 assembly at the cell surface.

Whatever the reason for the affinity of HIV-1 to macrophage internal compartments is, the results of this thesis demonstrate the advantage of sequestration into internal VCCs: although some VCCs might be connected to the plasma membrane and can be targeted by very small dyes, macrophage internal HIV-1 is protected from neutralizing antibodies, but can be very efficiently transferred to CD4+ T-cells by the establishment of virological synapses. Cell-to-cell transfer seems to be the main infection route *in vivo*, in which the majority of viral spread takes place in lymphatic organs (Martin et al., 2010). By this immune evasion mechanism and its long lifetime macrophages might serve as robust viral factories and cellular reservoirs for the virus. While the immune system tries to suppress cell free virus, HIV-1 replicates and persists at low levels in macrophages, protected from antibodies, but ready to infect new target cells. During the circulation through tissues infected macrophages disseminate HIV-1 into the CNS by crossing the blood-brain barrier (Maung et al., 2011; Waki and Freed, 2010). In this privileged tissue, the clearance of the virus is hardly feasible and cytopathic effects lead to neuronal destructions which cannot be prevented by antiretroviral therapy (Schnell et al., 2011).

The origin of VCCs in macrophages has to be addressed in further studies. However it is clear that the inaccessibility of HIV-1 in macrophages towards neutralizing antibodies will complicate vaccine development. An effective vaccine has to boost the cellular immune system instead of the humoral immune response. Most importantly cytotoxic T-cells should be able to detect and kill infected cells, including macrophages, memory T-cells and other cellular reservoirs. Thus, there is a need for new drugs which are able to destroy infected cellular reservoirs including macrophages, especially in the CNS. In this context further investigation in HIV-1 Gag synthesis in macrophages is important, since Gag has been shown to be the main player in hijacking the cellular system and expanding the

assembly platform in macrophages. It is worth to remember that there are ART-drugs acting against reverse transcriptase, protease, integrase and viral entry. In contrast, no drug blocking HIV-1 Gag function is available. More comprehensive investigations concerning the assembly process of HIV-1 and the cellular cofactors, including tetraspanins, will give information how to inhibit the function of HIV-1 Gag.



## 7 References

**AIDS Epidemic Update:** November 2009.

**Alexaki, A., Liu, Y., and Wigdahl, B.** (2008) Cellular Reservoirs of HIV-1 and their Role in Viral Persistence. *Curr HIV Res* 6:388-400.

**Allers, K., Hütter, G., Hofmann, J., Loddenkemper, C., Rieger, K., Thiel, E., and Schneider, T.** (2011) Evidence for the cure of HIV infection by CCR5D32/D32 stem cell transplantation. *Blood* 117:2791-2799.

**Bailes, E., Gao, F., Bibollet-Ruche, F., Courgnaud, V., Peeters, M., Marx, P.A., Hahn, B.H., and Sharp, P.M.** (2003) Hybrid origin of SIV in chimpanzees. *Science* 300:1713.

**Banning, C., Votteler, J., Hoffmann, D., Koppensteiner, H., Warmer, M., Reimer, R., Kirchhoff, F., Schubert, U., Hauber, J., and Schindler, M.** (2010) A flow cytometry-based FRET assay to identify and analyse protein-protein interactions in living cells. *PLoS One* 5:e9344.

**Barré-Sinoussi, F., Chermann, J.C., Rey, F., Nugeyre, M.T., Chamaret, S., Gruest, J., Dautet, C., Axler-Blin, C., Vezinét-Brun, F., Rouzioux, C., Rozenbaum, W., and Montagnier, L.** (1983) Isolation of a T-lymphotropic retrovirus from a patient at risk for AIDS. *Science* 220:868-871.

**Benaroch, P., Billard, E., Gaudin, R., Schindler, M., and Jouve, M.** (2010) HIV-1 assembly in macrophages. *Retrovirology* 7:29.

**Bennett, A. E., Narayan, K., Shi, D., Hartnell, L.M., Gouset, K., He, H., Lowekamp, B.C., Yoo, T.S., Bliss, D., Freed, E.O., and Subramaniam, S.** (2009) Ion-abrasion scanning electron microscopy reveals surface-connected tubular conduits in HIV-infected macrophages. *PLoS Pathog* 5:e1000591.

**Bieniasz, P. D.** (2009) The cell biology of HIV-1 virion genesis. *Cell Host Microbe* 5:550-558.

**Brandt, S. M., Mariani, R., Holland, A.U., Hope, T.J., and Landau, N.R.** (2002) Association of chemokine-mediated block to HIV entry with coreceptor internalization. *The Journal of biological chemistry* 277:17291-17299.

**Cao, H., and Walker, B.D.** (2000) Immunopathogenesis of HIV-1 Infection. *Clin Dermatol* 18:401-410

**Carl, S., Greenough, T.C., Krumbiegel, M., Greenberg, M., Skowronski, J., Sullivan, J.L., Kirchhoff, F.** (2001) Modulation of different human immunodeficiency virus type 1 Nef functions during progression to AIDS. *J Virol* 75:3657-3665.

- Carr, J. M., Hocking, H., Li, P., and Burrell, C.J.** (1999) Rapid and efficient cell-to-cell transmission of human immunodeficiency virus infection from monocyte-derived macrophages to peripheral blood lymphocytes. *Virology* 265:319-329.
- Carter, C.A., and Ehrlich, L.S.** (2008) Cell Biology of HIV-1 Infection of Macrophages. *Annu Rev Microbiol* 62:425-443.
- Charrin, S., le Naour, F., Silvie, O., Milhiet, P.E., Boucheix, C., and Rubinstein E.** (2009) Lateral organization of membrane proteins: tetraspanins spin their web. *Biochem J* 420:133-154.
- Chertova, E., Chertov, O., Coren, L.V., Roser, J.D., Trubey, C.M., Bess, J.W. Jr., Sowder, R.C. 2nd, Barsov, E., Hood, B.L., Fisher, R.J., Nagashima, K., Conrads, T.P., Veenstra, T.D., Lifson, J.D., and Ott, D.E.** (2006) Proteomic and biochemical analysis of purified human immunodeficiency virus type 1 produced from infected monocyte-derived macrophages. *J Virol* 80:9039–9052.
- Clavel, F., Guyader, M., Guetard, D., Salle, M., Montagnier, L., and Alizon, M.** (1986) Molecular cloning and polymorphism of the human immune deficiency virus type 2. *Nature* 324:691-695.
- Clay, C.C., Rodrigues, D.S., Ho, Y.S., Fallert, B.A., Janatpour, K., Reinhart, T.A., and Esser, U.** (2007) Neuroinvasion of fluorescein-positive monocytes in acute simian immunodeficiency virus infection. *J Virol* 81:12040-12048.
- Coffin, J., Haase A., Levy J.A., Montagnier L., Oroszlan S., Teich N., Temin H., Toyoshima K., Varmus H. and Vogt P.L.** (1986) What to call the AIDS virus? *Nature* 321:10.
- Connor, R.I., Mohri, H., Cao, Y., and Ho, D.D.** (1993) Increased viral burden and cytopathicity correlate temporally with CD41 Tlymphocyte decline and clinical progression in human immunodeficiency virus type 1-infected individuals. *J Virol* 67:1772–1777.
- De Cock, K.M., Jaffe, H.W., and Curran, J.W.** (2011) Reflections on 30 years of AIDS. *Emerg Infect Dis* 17:1044-1048.
- Dean, M., Carrington, M., Winkler, C., Huttley, G.A., Smith, M.W., Allikmets, R., Goedert, J.J., Buchbinder, S.P., Vittinghoff, E., Gomperts, E., Donfield, S., Vlahov, D., Kaslow, R., Saah, A., Rinaldo, C., Detels, R., and O'Brien, S.J.** (1996) Genetic restriction of HIV-1 infection and progression to AIDS by a deletion allele of the CKR5 structural gene. Hemophilia Growth and Development Study, Multicenter AIDS Cohort Study, Multicenter Hemophilia Cohort Study, San Francisco City Cohort, ALIVE Study. *Science* 273:1856–1862.

- Deneka, M., Pelchen-Matthews A., Byland R., Ruiz-Mateos E., and Marsh M.** (2007) In macrophages, HIV-1 assembles into an intracellular plasma membrane domain containing the tetraspanins CD81, CD9, and CD53. *J Cell Biol* 177:329-341.
- DuBridgE, R.B., Tang, P., Hsia, H.C., Leong, P.M., Miller, J.H., and Calos, M.P.** (1987) Analysis of mutation in human cells by using an Epstein-Barr virus shuttle system. *Mol Cell Biol* 7:379-387.
- Engering, A. and Pieters, J.** (2001) Association of distinct tetraspanins with MHC class II molecules at different subcellular locations in human immature dendritic cells. *Int Immunol* 13:127-134.
- Favoreel, H. W., Van Minnebruggen, G., Van de Walle, G.R., Ficinska, J., and Nauwynck H.J.** (2006) Herpesvirus interference with virus-specific antibodies: bridging antibodies, internalizing antibodies, and hiding from antibodies. *Vet Microbiol* 113:257-263.
- Fouchier, R.A., Meyer, B.E., Simon, J.H., Fischer, U., and Malim, M.H.** (1997) HIV-1 infection of non-dividing cells: evidence that the amino-terminal basic region of the viral matrix protein is important for Gag processing but not for post-entry nuclear import. *EMBO J* 16:4531-4539.
- Frankel, A.D., and Young, J.A.** (1998) HIV-1: Fifteen Proteins and an RNA. *Annu Rev Biochem* 67:1-25.
- Ganesh, L., Leung, K., Lore, K., Levin, R., Panet, A., Schwartz, O., R. A. Koup, R.A., and Nabel, G.J.** (2004) Infection of specific dendritic cells by CCR5-tropic human immunodeficiency virus type 1 promotes cell-mediated transmission of virus resistant to broadly neutralizing antibodies. *J Virol* 78:11980-11987.
- Gendelman, H.E., Orenstein, J.M., Martin, M.A., Ferrua, C., Mitra, R., Phipps, T., Wahl, L.A., Lane, H.C., Fauci, A.S., Burke, D.S., Skillman, D., and Meltzeri, M.S.** (1988) Efficient isolation and propagation of human immunodeficiency virus on recombinant colony-stimulating factor 1-treated monocytes. *J Exp Med* 167:1428-1441.
- Gordon, S., and Taylor, P.R.** (2005) Monocyte and macrophage heterogeneity. *Nat Rev Immunol* 5:953-964.
- Gould, S.J., Booth, A.M., and Hildreth, J.E.** (2003) The Trojan exosome hypothesis. *Proc Natl Acad Sci USA* 100:10592-10597.
- Gousset, K., Ablan, S.D., Coren, L.V., Ono, A., Soheilian, F., Nagashima, K., Ott, D.E., and Freed, E.O.** (2008) Real-time visualization of HIV-1 GAG trafficking in infected macrophages. *PLoS Pathog* 4:e1000015.

- Grewe, B., and Überla, K.** (2010) The human immunodeficiency virus type 1 Rev protein: ménage à trois during the early phase of the lentiviral replication cycle. *J Gen Virol* 91:1893-1897.
- Grigorov, B., Attuil-Audenis, V., Perugi, F., Nedelec, M., Watson, S., Pique, C., Darlix, J.L., Conjeaud, H., and Muriaux D.** (2009) A role for CD81 on the late steps of HIV-1 replication in a chronically infected T cell line. *Retrovirology* 6:28.
- Groot, F., Welsch, S., and Sattentau, Q.J.** (2008) Efficient HIV-1 transmission from macrophages to T cells across transient virological synapses. *Blood* 111:4660-4663.
- Gulick, R.M., Lalezari, J., Goodrich, J., Clumeck, N., DeJesus, E., Horban, A., Nadler, J., Clotet, B., Karlsson, A., Wohlfeiler, M., Montana, J.B., McHale, M., Sullivan, J., Ridgway, C., Felstead, S., Dunne, M.W., Wohlfeiler, M., Montana, J.B., McHale, M., Van der Ryst, E., and Mayer, H.** (2008) Maraviroc for Previously Treated Patients with R5 HIV-1 Infection. *N Engl J Med* 359:1429-1441.
- He, N., and Zhou, Q.** (2011) New Insights into the Control of HIV-1 Transcription: When Tat Meets the 7SK snRNP and Super Elongation Complex (SEC). *J Neuroimmune Pharmacol* 6:260-268.
- Hoffmann, C., Rockstroh, J.K., and Kamps, B.S.** (2008) HIV.net 2008. [www.hiv.net](http://www.hiv.net)
- Ho, S. H., Martin, F., Higginbottom, A., Partridge, L.J., Parthasarathy, V., Moseley, G.W., Lopez, P., Cheng-Mayer, C., and Monk, P.N.** (2006) Recombinant extracellular domains of tetraspanin proteins are potent inhibitors of the infection of macrophages by human immunodeficiency virus type 1. *J Virol* 80:6487-6496.
- Hogue, I. B., Grover, J.R., Soheilian, F., Nagashima, K., and Ono, A.** (2011) Gag Induces the Coalescence of Clustered Lipid Rafts and Tetraspanin-Enriched Microdomains at HIV-1 Assembly Sites on the Plasma Membrane. *J Virol* 85:9749-9766.
- Hübner, W., Chen, P., Del Portillo, A., Liu, Y., Gordon, R.E., and Chen, B.K.** (2007) Sequence of human immunodeficiency virus type 1 (HIV-1) Gag localization and oligomerization monitored with live confocal imaging of a replication-competent, fluorescently tagged HIV-1. *J Virol* 81:12596-12607.
- Hübner, W., McNerney, G.P., Chen, P., Dale, B.M., Gordon, R.E., Chuang, F.Y., Li, X.D., Asmuth, D.M., Huser, T., and Chen, B.K.** (2009) Quantitative 3D video microscopy of HIV transfer across T cell virological synapses. *Science* 323:1743-1747.
- Hütter, G., Nowak, D., Mossner, M., Ganepola, S., Müßig, A., Allers, K., Schneider, T., Hofmann, J., Kücherer, C., Blau, O., W. Blau, I.W., Hofmann, W.K. and Thiel, E.** (2009) Long-term

control of HIV by CCR5 Delta32/Delta32 stemcell transplantation. *N Engl J Med* 360:692-698.

**Ivanchenko, S., Godinez, W.J., Lampe, M., Krausslich, H.G., Eils, R., Rohr, K., Brauchle, C., Muller, B., and Lamb, D.C.** (2009). Dynamics of HIV-1 assembly and release. *PLoS Pathog* 5, e1000652.

**Jolly, C., and Sattentau, Q.J.** (2007) Human immunodeficiency virus type 1 assembly, budding, and cell-cell spread in T cells take place in tetraspanin-enriched plasma membrane domains. *J Virol* 81:7873-7884.

**Joshi, A., Ablan, S.D., Soheilian, F., Nagashima, K., and Freed, E.O.** (2009) Evidence that productive human immunodeficiency virus type 1 assembly can occur in an intracellular compartment. *J Virol* 83:5375-5387.

**Jouve, M., Sol-Foulon, N., Watson, S., Schwartz, O., and Benaroch, P.** (2007) HIV-1 buds and accumulates in "nonacidic" endosomes of macrophages. *Cell Host Microbe* 2:85-95.

**Jouvenet, N., Neil, S.J., Bess, C., Johnson, M.C., Virgen, C.A., Simon, S.M., and Bieniasz, P.D.** (2006) Plasma membrane is the site of productive HIV-1 particle assembly. *PLoS Biol* 4:e435.

**Kahn, J.O., and Walker, B.D.** (1998) Acute human immunodeficiency virus type-1 infection. *N Engl J Med* 339:33-39.

**Krementsov, D.N., Weng, J., Lambele, M., Roy, N.H. and Thali, M.** (2009) Tetraspanins regulate cell-to-cell transmission of HIV-1. *Retrovirology* 6:64.

**Khurana, S., Krementsov, D.N., de Parseval, A., Elder, J.H., Foti, M., and Thali, M.** (2007) Human immunodeficiency virus type 1 and influenza virus exit via different membrane microdomains. *J Virol* 81:12630-12640.

**Kwon, D.S., Gregorio, G., Bitton, N., Hendrickson, W.A., and Littman, D.R.** (2002) DC-SIGN-mediated internalization of HIV is required for trans-enhancement of T cell infection. *Immunity* 16:135-144.

**Laguet, N., Sobhian, B., Casartelli, N., Ringeard, M., Chable-Bessia, C., Ségéral, E., Yatim, A., Emiliani, S., Schwartz, O., and Benkirane, M.** (2011) SAMHD1 is the dendritic- and myeloid-cell-specific HIV-1 restriction factor counteracted by Vpx. *Nature* 474:654-657.

**Law, M., Hollinshead, R., and Smith, G.L.** (2002) Antibody-sensitive and antibody-resistant cell-to-cell spread by vaccinia virus: role of the A33R protein in antibody-resistant spread. *J Gen Virol* 83:209-222.

- Le Douce, V., Herbein, G., Rohr, O., and Schwartz, C.** (2010) Molecular mechanisms of HIV-1 persistence in the monocyte-macrophage lineage. *Retrovirology* 7:3.
- Maniatis, T., Sambrook, J., and Fritsch, E. F.** (1989). Molecular cloning. *Cold Spring Harbor laboratory Press, New York.*
- Marsh, M., Theusner, K., and Pelchen-Matthews, A.** (2009) HIV assembly and budding in macrophages. *Biochem Soc Trans* 37:185-189.
- Martin, F., Roth, D.M., Jans, D.A., Pouton, C.W., Partridge, L.J., Monk, P.N., and Moseley, G.W.** (2005) Tetraspanins in Viral Infections: a Fundamental Role in Viral Biology? *J Virol* 79:10839-10851.
- Martin, M., Welsch, S., Jolly, C., Briggs, J.A., Vaux, D., and Sattentau, Q.J.** (2010) Virological synapse-mediated spread of human immunodeficiency virus type 1 between T cells is sensitive to entry inhibition. *J Virol* 84:3516–3527.
- Mattheyses, A.L., Simon, S.M., and Rappoport, J.Z.** (2010) Imaging with total internal reflection fluorescence microscopy for the cell biologist. *Cell Sci* 123:3621-3628.
- Maung, R., Medders, K.E., Sejbuk, N.E., Desai, M.K., Russo, R., and Kaul, M.** (2011) Genetic Knockouts Suggest a Critical Role for HIV Co-Receptors in Models of HIV gp120-Induced Brain Injury. *J Neuroimmune Pharmacol* In press.
- McDonald, D., Wu, L., Bohks, S.M., KewalRamani, V.N., Unutmaz, D., and Hope, T.J.** (2003) Recruitment of HIV and its receptors to dendritic cell-T cell junctions. *Science* 300:1295–1297.
- Mellors, J.W., Rinaldo, C.R.J., Gupta, P., White, R.M., Todd, J.A., Kingsley, L.A.** (1997) Prognosis in HIV-1 infection predicted by the quantity of virus in plasma. *Science* 275:1167–1170.
- Monini, P., Sgadari, C., Toschi, E., Barillari, G., and Ensoli, B.** (2004) Antitumour effects of antiretroviral therapy. *Nat Rev Cancer* 4:861-875.
- Muller, B., Daecke, J., Fackler, O.T., Dittmar, M.T., Zentgraf, H., and Krausslich, H.G.** (2004) Construction and characterization of a fluorescently labeled infectious human immunodeficiency virus type 1 derivative. *J Virol* 78:10803-10813.
- Nguyen, D.G., Booth, A., Gould, S.J., and Hildreth, J.E.** (2003) Evidence that HIV budding in primary macrophages occurs through the exosome release pathway. *J Biol Chem* 278:52347–52354.

- Nydegger, S., Khurana, S., Kremontsov, D.N., Foti, M., and Thali, M.** (2006) Mapping of tetraspanin-enriched microdomains that can function as gateways for HIV-1. *J Cell Biol* 173:795–807.
- Ochsenbauer-Jambor, C., Jones, J., Heil, M., Zammit, K.P., and Kutsch, O.** (2006) T-cell line for HIV drug screening using EGFP as a quantitative marker of HIV-1 replication. *Biotechniques* 40:91-100.
- Ono, A.** (2009) HIV-1 Assembly at the Plasma Membrane: Gag Trafficking and Localization. *Future Virol* 4:241-257.
- Orenstein, J. M., Meltzer, M.S., Phipps, T., and Gendelman, H.E.** (1988) Cytoplasmic assembly and accumulation of human immunodeficiency virus types 1 and 2 in recombinant human colony-stimulating factor-1-treated human monocytes: an ultrastructural study. *J Virol* 62:2578-2586.
- Pantaleo, G., Graziosi, C., and Fauci, A.S.** (1993) The immunopathogenesis of human immunodeficiency virus infection. *N Engl J Med* 328:327–335.
- Papkalla, A., Munch, J., Otto, C., and Kirchhoff, F.** (2002) Nef enhances human immunodeficiency virus type 1 infectivity and replication independently of viral coreceptor tropism. *J Virol* 76:8455-8459.
- Pelchen-Matthews, A., Kramer, B., and Marsh, M.** (2003) Infectious HIV-1 assembles in late endosomes in primary macrophages. *J Cell Biol* 162:443-455.
- Phillips, D. M., Tan, X., Perotti, M.E., and Zacharopoulos, V.R.** (1998) Mechanism of monocyte-macrophage-mediated transmission of HIV. *AIDS research and human retroviruses* 1:67-70.
- Pierson, T., McArthur, J., and Siliciano, R.F.** (2000) Reservoirs for HIV-1: Mechanisms for Viral Persistence in the Presence of Antiviral Immune Responses and Antiretroviral Therapy. *Annu Rev Immunol* 18:665-708.
- Raposo, G., Moore, M., Innes, D., Leijendekker, R., Leigh-Brown, A., Benaroch, P., and Geuze, H.** (2002) Human macrophages accumulate HIV-1 particles in MHC II compartments. *Traffic* 3:718-729.
- Ruiz-Mateos, E., Pelchen-Matthews, A., Deneka, M., and Marsh, M.** (2008) CD63 Is Not Required for Production of Infectious Human Immunodeficiency Virus Type 1 in Human Macrophages. *J Virol* 82:4751-4761.

- Saiki, R.K., Gelfand, D.H., Stoffel, S., Scharf, S.J., Higuchi, R., Horn, G.T., Mullis, K.B., and Erlich, H.A.** (1988) Primer-directed enzymatic amplification of DNA with a thermostable DNA polymerase. *Science* 239:487-491.
- Schindler, M., Wurfl, S., Benaroch, P., Greenough, T. C., Daniels, R., Easterbrook, P., Brenner, M., Munch, J., Kirchhoff, F.** (2003). Down-modulation of mature major histocompatibility complex class II and up-regulation of invariant chain cell surface expression are well-conserved functions of human and simian immunodeficiency virus nef alleles. *J.Virol* 77:10548-10556.
- Schindler, M., Wildum, S., Casartelli, N., Doria, M., and Kirchhoff, F.** (2007) Nef alleles from children with non-progressive HIV-1 infection modulate MHC-II expression more efficiently than those from rapid progressors. *AIDS* 21:1103-1107.
- Schindler, M., Rajan, D., Banning, C., Wimmer, P., Koppensteiner, H., Iwanski, A., Specht, A., Sauter, D., Dobner, T., and Kirchhoff, F.** (2010) Vpu serine 52 dependent counteraction of tetherin is required for HIV-1 replication in macrophages, but not in ex vivo human lymphoid tissue. *Retrovirology* 7:1.
- Schnell, G., Joseph, S., Spudich, S., Price, R.W., and Swanstrom, R.** (2011) HIV-1 Replication in the Central Nervous System Occurs in Two Distinct Cell Types. *PLoSPathog* 7(10): e1002286.
- Sharova, N., Swingler, C., Sharkey, M., and Stevenson, M.** (2005) Macrophages archive HIV-1 virions for dissemination in trans. *Embo J* 24:2481-2489.
- Sharp, P.M., and Hahn, B.H.** (2011) Origins of HIV and the AIDS Pandemic. *Cold Spring Harb Perspect Med* 1:a006841.
- Singethan, K., Müller, N., Schubert, S., Lüttge, D., Kremmentsov, D.N., Khurana, S.R., Krohne, G., Schneider-Schaulies, S., Thali, M., and Schneider-Schaulies, J.** (2008) CD9 clustering and formation of microvilli zippers between contacting cells regulates virus-induced cell fusion. *Traffic* 9:924–935.
- Spijkerman, I., de Wolf, F., Langendam, M., Schuitemaker, H., and Coutinho, R.** (1998) Emergence of syncytium-inducing human immunodeficiency virus type 1 variants coincides with a transient increase in viral RNA level and is an independent predictor for progression to AIDS. *J Infect Dis* 178:397–403.
- Tarrant, J.M., Robb, L., van Spriel, A.B., and Wright, M.D.** (2003) Tetraspanins: molecular organisers of the leukocyte surface. *Trends Immunol* 24:610-617.



- Thali, M.** (2011) Tetraspanin functions during HIV-1 and influenza virus replication. *Biochem Soc Trans* 39:529–531.
- Thompson, K.A., Varrone, J.J., Jankovic-Karasoulos, T., Wesselingh, S.L., and McLean, C.A.** (2009) Cell specific temporal infection of the central nervous system in a simian immunodeficiency virus model of human immunodeficiency virus encephalitis. *J Neurovirol* 15:300–311.
- Thompson, K.A., Cherry, C.L., Bell, J.E., and McLean, C.A.** (2011) Brain Cell Reservoirs of Latent Virus in Presymptomatic HIV-Infected Individuals. *Am J Pathol* 179:1623–1629.
- Timpe, J. M., Stamatakis, Z., Jennings, A., Hu, K., Farquhar, M.J., Harris, H.J., Schwarz, A., Desombere, I., Roels, G.L., Balfe, P., and McKeating, J.A.** (2008) Hepatitis C virus cell-cell transmission in hepatoma cells in the presence of neutralizing antibodies. *Hepatology* 47:17–24.
- Trkola, A., Purtscher, M., Muster, T., Ballaun, C., Buchacher, A., Sullivan, N., Srinivasan, K., Sodroski, J., Moore, J.P., and Katinger, H.** (1996) Human monoclonal antibody 2G12 defines a distinctive neutralization epitope on the gp120 glycoprotein of human immunodeficiency virus type 1. *J Virol* 70:1100-1108.
- UNAIDS Report.** (2010) UNAIDS Report on the global AIDS Epidemic.
- van Montfort, T., Nabatov, A.A., Geijtenbeek, T.B., Pollakis, G., and Paxton, W.A.** (2007) Efficient capture of antibody neutralized HIV-1 by cells expressing DC-SIGN and transfer to CD4 T lymphocytes. *J. Immunol* 178:3177–3185.
- von Lindern, J. J., Rojo, D., Grovit-Ferbas, K., Yeramian, C., Deng, C., Herbein, G., Ferguson, M.R., Pappas, T.C., Decker, J.M., Singh, A., Collman, R.G., and O'Brien, W.A.** (2003) Potential role for CD63 in CCR5-mediated human immunodeficiency virus type 1 infection of macrophages. *J. Virol* 77:3624–3633.
- Waki, K., and Freed, E.O.** (2010) Macrophages and Cell-Cell Spread of HIV-1. *Viruses* 574 2:1603-1620
- Welsch, S., Keppler, O.T., Habermann, A., Allespach, I., Krijnse-Locker, J., and Kräusslich, H.G.** (2007) HIV-1 buds predominantly at the plasma membrane of primary human macrophages. *PLoS Pathog* 3(3): e36.
- Welsch, S., Groot, F., Krausslich, H.G., Keppler, O.T., and Sattentau, Q.T.** (2011) Architecture and Regulation of the HIV-1 Assembly and Holding Compartment in Macrophages. *Journal of virology* 85:7922-7927.

**Wildum, S., Schindler, M., Munch, J., and Kirchhoff, F.** (2006). Contribution of Vpu, Env, and Nef to CD4 down-modulation and resistance of human immunodeficiency virus type 1-infected T cells to superinfection. *J Virol* 80:8047-8059.

**Wu, X., Yang, Z.Y., Li, Y., HogerCorp, C.M., Schief, W.R., Seaman, M.S., Zhou, T., Schmidt, S.D., Wu, L., Xu, L., Longo, N.S., McKee, K., O'Dell, S., Louder, M.K., Wycuff, D.L., Feng, Y., Nason, M., Doria-Rose, N., Connors, M., Kwong, P.D., Roederer, M., Wyatt, R.T., Nabel, G.J., and Mascola, J.R.** (2010) Rational design of envelope identifies broadly neutralizing human monoclonal antibodies to HIV-1. *Science* 329:856-861.

## List of Figures

Figure 1.1	Global prevalence of HIV-1.	7
Figure 1.2	Structure and genome organization of HIV-1.	8
Figure 1.3	Replication cycle of HIV-1.	9
Figure 1.4	Typical course of HIV-1 infection.	11
Figure 6.1	Schematic genome organization of HIV-1 Gag-iGFP (HIV-1 GG).	33
Figure 6.2	GFP expression resembles Gag distribution in HIV-1 GG-infected macrophages.	34
Figure 6.3	Gag accumulations and sites of HIV-1 assembly in HIV-1 infected cells.	35
Figure 6.4	Characterization of R5-tropic HIV-1 NL4-3 Gag-iGFP (HIV-1 GG).	35
Figure 6.5	Representative 3-D reconstruction of GFP/Gag distribution in HIV-1 GG-infected MDM.	36
Figure 6.6	Representative Live Cell Imaging of HIV-1 GG-infected MDM.	37
Figure 6.7	Kinetics of Gag expression in HIV-1 GG-infected MDM.	38
Figure 6.8	Four-dimensional time lapse of an HIV-1 GG-infected macrophage.	39
Figure 6.9	Schematic presentation of Total internal reflection fluorescence technique.	40
Figure 6.10	TIRF analysis of HIV-1 GG infected macrophages and 293T cells.	40
Figure 6.11	TIRF analysis of HIV-1 GG infected macrophages and 293T cells.	41
Figure 6.12	FACS-FRET analysis of HIV-1 Gag with CD81, TfR, and CD4 in transfected 293T cells.	43
Figure 6.13	The Gag assembly compartment in HIV-1 infected MDM is not accessible to antibodies at 4°C.	44
Figure 6.14	HIV-1 within VCCs is protected from neutralizing antibodies.	45
Figure 6.15	Live Cell Imaging of HIV-1 GG transfer from MDM to PBMC.	46
Figure 6.16	Antibody preincubation does not suppress HIV-1 transfer from MDM to T-cells.	47
Figure 6.17	Correlative microscopy of macrophage internal HIV-1 accumulations.	48
Figure 6.18	Three-dimensional reconstruction of the serial EM sections of a VCC.	49
Figure 6.19	Expression of Gag-CFP in macrophages.	50
Figure 6.20	FACS-FRET analysis of HIV-1 Gag with the tetraspanins CD81, CD82, CD53 and CD9 which are located in VCC.	51

## Abbreviations

$\alpha$	antibody against ...
°C	degree Celsius
$\mu$ l	microliter
$\mu$ m	micrometer
29/31 KE	mutated HIV-1 matrix protein
2D/ 3D	two-dimensional / three-dimensional
AB	antibody
AIDS	acquired immunodeficiency syndrome
APC	antigen presenting cells
ART	antiretroviral therapies
CA/p24	HIV-1 capsid protein
CCR5/ CXCR4	chemokine receptor type 5 / 4
CCR5 $\Delta$ 32	deletion of 32 base pairs in the CCR5 gene
CD (4)	cluster of differentiation (4)
CDC	Center of Disease Control and Prevention
cDNA	complementary DNA
CFP	cyan fluorescent protein
CMV	<i>Cytomegalovirus</i>
CNS	central nervous system
DC	dendritic cells
ddH <sub>2</sub> O	double distilled water
DEPC	diethylpyrocarbonat
DIC	differential interference contrast
DMEM	Dulbecco's modified Eagle Medium
DMSO	dimethyl sulfoxide
DNA	deoxyribonucleic acid
dNTP	deoxyribonucleotide
dpc	days post coculture
dpi	days post infection
<i>E.coli</i>	<i>Escherichia coli</i>
e.g.	example given
EDTA	ethylen-diamin-tetraacetat
EGFR	epidermal growth factor receptor
ELISA	enzyme-linked immunosorbent assay
EM	electron microscopy
Env/ Gp160	HIV-1 envelope
FACS	fluorescence-activated cell sorting
FCS	fetal Craft's serum
FRET	Förster resonance energy transfer
g	gram
g/L	gram per liter
GA	glutaraldehyde
Gag	HIV-1 group specific antigen
GFP	green fluorescent protein

Gp	glycoprotein
h	hour
H <sub>2</sub> O	water
HAD	HIV associated dementia
HAND	HIV associated neurocognitive disorders
HBS	HEPES buffered saline
HEK	human kidney epithelial cell
HIV-1	<i>Human Immunodeficiency Virus Type 1</i>
HIV-1 GC	pBR-NL4-3-V3 92th014.12_Gag-iCFP
HIV-1 GG	pBR-NL4-3-V3 92th014.12_Gag-iGFP
HIVE	HIV encephalitis
hpi	hours post infection
HRP	horseradish peroxidase
IA-SEM	ion-abrasion scanning electron microscopy
Ig	immunoglobulin
IN/ pol3	HIV-1 integrase
kb	kilo bases
kV	kilovolt
LB	Luria-Bertani-
LCI	Leibniz Center of Infection
LTR	long terminal repeats
M	mol
MA/ p17	HIV-1 matrix protein
MDM	monocyte derived macrophages
MHC-I or II	major histocompatibility complex-1 or 2
min	minutes
mio	million
M&M	material and methods
mmol	millimol
Mr	molecular weight
ms	milliseconds
MVB	multi vesicular bodies
NA	numerical aperture
NC/ p7	HIV-1 nuclear capsid protein
Nef	HIV-1 negative factor
nm	nanometer
non perm.	not permeabilized
NS	not significant
PBL	peripheral blood lymphocytes
PBMC	peripheral blood mononuclear cells
PBS	phosphate buffered saline
PCR	polymerase-chain-reaction
perm.	permeabilized
PFA	paraformaldehyde
PIC	preintegration complex
PM	plasma membrane
Pol	HIV-1 polymerase polyprotein

PR/ pol 1	HIV-1 protease
R	Pearson's correlation coefficient
R2	squared Pearson's correlation coefficient
R5	CCR5 tropic
Rev	HIV-1 regulator of expression of virion proteins
RNA	ribonucleic acid
ROI	region of interest
RPMI	Roswell Park Memorial Institute
RR	ruthenium red
RT	HIV-1 reverse transcriptase
SAM-HD1	sterile alpha motif and HD domain 1
sec/ s	second
shRNA	small hairpin RNA
SIV	<i>Simian Immunodeficiency Virus</i>
SIVcpz	<i>Simian Immunodeficiency Virus</i> of chimpanzees
SU/ Gp120	HIV-1 surface protein
t	time
TAR	trans-activation response
Tat	transactivator of transcription
TC/ tetra-cys	tetracystein
TEM	tetraspanin enriched microdomains
TfR	transferrin receptor
Th2	T helper 2
TIRF	total internal reflection fluorescence
TM/ Gp41	HIV-1 transmembrane protein
UV	ultraviolet
v/v	volume per volume
VCC	virus containing compartments
Vif	HIV-1 viral infectivity factor
VLP	virus like particles
Vpr	HIV-1 viral protein rapid
Vpu	HIV-1 viral protein out
VS	virological synapse
VSV-G	glycoprotein G of <i>Vesicular Stomatitis Virus</i>
w/v	mass per volume
Wt	wild type
X4	CXCR4 tropic
YFP	yellow fluorescent protein

## Danksagung

Besonders möchte ich mich an diese Stelle bei Dr. Michael Schindler für die Möglichkeit bedanken, dass ich meine Dissertation in der Nachwuchsgruppe Viruspathogenese (AG76) am Heinrich-Pette-Institut anfertigen durfte. Ich bedanke mich für die hervorragende Betreuung, die hilfreichen Diskussionen, für das Korrekturlesen dieser Arbeit, für die Unterstützung und für das in mich gesetzte Vertrauen. Vielen Dank für die Möglichkeit meine Daten auf internationalen Kongressen präsentieren zu dürfen und dass ich dieses interessante Thema bearbeiten durfte.

Weiterhin möchte ich besonders meinem Doktorvater Prof. Dr. Thomas Dobner danken; auch für die Möglichkeit meine Arbeit in der Gruppe Molekulare Virologie (Abteilung 1) abschließen zu dürfen, nachdem Dr. Schindler ans Helmholtz-Zentrum-München gewechselt ist.

PD Dr. Nicole Fischer danke ich ebenfalls herzlich für die freundliche Übernahme des Zweitgutachtens dieser Arbeit und dass sie mich im Rahmen des LCI-Graduierten-Kollegs als Kobetreuerin unterstützt hat. Auch sei hier mein Dank an Prof. Dr. Hans Will und Prof. Dr. Udo Wienand gerichtet, die die Begutachtung meiner Disputation übernehmen, an Prof. Dr. Alexander Haas als Vorsitzenden sowie an alle Fragesteller.

Mein Dank gilt weiters der Forschungsgruppe Elektronenmikroskopie ohne deren aktive Mitarbeit durch Erstellung der EM-Aufnahmen und die vielfachen Tipps und Hilfen bei allen Mikroskopiefragen ein Gelingen dieser Arbeit nicht möglich gewesen wäre. Vor allem danke ich auch Dr. Heinrich Hohenberg, Carola Schneider, Dr. Rudolph Reimer, Martin Warmer und Barbara Holstermann.

Vor allem danke ich natürlich allen meinen Kolleginnen und Kollegen aus der AG76 und der Abteilung 1, auch denen, die nicht mehr am Institut sind, für das tolle Arbeitsklima im Labor, ihre Hilfe und für zahlreiche lustige Abende außerhalb der Forschung!

Bedanken möchte ich mich hier gesondert nochmals bei Carina, die mich über fast drei Jahren als liebe, hilfsbereite Kollegin unterstützt und in viele wissenschaftliche Methoden eingeschult hat.

Großer Dank gilt auch meiner Familie – vor allem der Unterstützung meiner Mutter Ines und meines Bruders Wolfram.

Mein ganz besonderer Dank richtet sich an meine Heidelinde, die mich nach Hamburg begleitet hat, mich bei allem unterstützt, immer hinter mir steht und volles Verständnis zeigte, wenn es im Labor mal länger wurde oder wenn das gemeinsame Wochenende für die Arbeit geopfert werden musste.

## **Eidesstattliche Erklärung**

Hiermit erkläre ich, dass ich bisher keine Promotionsversuche unternommen habe. Weiterhin versichere ich, dass ich die vorliegende Arbeit selbstständig durchgeführt und keine anderen als die angegebenen Hilfsmittel verwendet habe.

Herwig Koppensteiner

Hamburg, 11. Mai 2012